DESIGN AND DEVELOPMENT OF CHESTNUT HARVESTING TECHNIQUES

By

Mark E. De Kleine

A THESIS

Submitted to
Michigan State University
in partial fulfillment of the requirements
for the degree of

MASTER OF SCIENCE

Biosystems Engineering

2011

ABSTRACT

DESIGN AND DEVELOPMENT OF CHESTNUT
HARVESTING TECHNIQUES

By

Mark E. De Kleine

A harvesting technique applicable for small chestnut orchards was designed and tested for chestnuts. The originality of the technique was a single-stage vacuum and separation process. A harvesting chamber was designed with inline obstructions which separate chestnuts from debris. The chestnuts were sorted into a deposit chamber and debris and waste was discharged to the environment.

Tests were made to determine chestnut harvesting performance as affected by the proportion of chestnuts to debris, and the feed rate into the system. The validation of the harvesting process was characterized by chestnut loss and separation efficiency. The quantity of chestnuts and the feed rate interaction significantly affected the harvesting performance parameters. Chestnut losses were as low as 1.3% while the separation efficiency was as high as 81%.

ACKNOWLEDGMENTS

Agriculture has been a part of my life, all of my life. My first exposure to the media was sitting on a giant pumpkin in Grand Haven, MI, when I was 3 or 4 years old. My experience with orchards and machinery has led me through many exciting adventures in Agricultural Engineering, including this. I received my B.S. in Biosystems Engineering from Michigan State University in the Spring of 2005. Six years later, I have had the fortunate, and unique, opportunity to re-walk those steps with the help of some amazing people.

I would like to express my appreciation and thanks to the flowing people who contributed to this project:

Dr. D. Guyer, who as my major professor provided insight, supervision, and assistance throughout this entire project,

Dr. A. Srivastava, Dr. C. Radcliffe, and Dr. D. Fulbright, for providing guidance and encouragement as a committee in both graduate studies and personal growth,

Dr. G. Van Ee and Dr. F. Bakker-Arkema, for their personal mentorship and advice,

De Kleine Orchards LLC., Chestnut Growers Inc., MSU's Biosystems and Agricultural Engineering Services staff, Mr. Jaime Burns, Mr. Irwin Donis-Gonzales, Mr. Mario Mujadanio and Ms. Lindsey S. New, for her support and exceptional knowledge of linguistics.

A small percentage of the world's population is involved in agriculture. Some sources say less than two percent of the population is responsible for feeding the rest. My far sighted goal for this project was to ultimately lay a foundation for engineering education. Those who understand engineering, at its' core, understand how engineering an educational system can benefit people everywhere. It is my dream that one day an engineered educational agriculture program will thrive in Michigan.

The picture of Sparty above my desk, signed by Sparty himself, reads:

dream BIG
-Sparty #1

Thank you for taking an interest in me, my thesis, and agricultural engineering!

Mark De Kleine

dekleine@msu.edu

Table of Contents

List of Tables viii

List of Figures ix

1 Introduction 1

2 Literature Review 2

3 Objective 4

4 Justification 5

5 Design Process 9
5.1 Separation Concepts and Strategies 9
5.1.1 Fluidized Beds 14
5.1.2 Cyclone Separation Systems 15
5.1.3 Physical Properties of Chestnuts and Burs 18
5.2 Machine Design 20
5.3 Platform 21
5.3.1 Frame and Engine/Fan drive 22
5.3.2 Tubing 23
5.3.3 Materials used for separation chambers 23

6 Iterative Designs 23
6.1 Procedure 24
6.2 Air Flow Separator 25
6.3 Dowel Grid Separator 27
6.4 Axial-Dowel Wheel Separator 31
6.5 Radial-Dowel Wheel Separator 34
6.6 Deflection Separator 37
6.7 Momentum Transfer Separator 39
6.8 Saltation Sieve Separator (SSS) 41

7 Experiment Design 44
7.1.1 Performance Evaluations 46

8 Results and Discussions 47
8.1 Chestnut Loss 48
8.2 Separation Efficiency 52

9 Conclusions 57

10 Future Research 57

APPENDICIES 59

11 Appendix A: Engine hp and Air Flow calculations 60

12 Appendix B: Velocity Profiles 63
12.1 B.1: Air Flow Separator 63
12.2 B.2: Dowel Grid Separator 69
12.3 B.3: Axial-Dowel Wheel Separator 73
12.4 B.4: Radial-Dowel Wheel Separator 76
12.5 B.5: Deflection Separator 76
12.6 B.6: Saltation Sieve Separator 76

REFERENCES 82

List of Tables

Table 1. Acreage estimated to economically afford a harvesting machine at various yields. For interpretation of the references to color in this, and all other figures, the reader is referred to the electronic version of this thesis. 9

Table 2. Reproduced from Marcus et al. 1990. 13

Table 3. Air velocities sufficient for vacuuming chestnuts, chestnuts in burs, and burs. Reproduced from Guyer and Kang (2009) 18

Table 4. Physical properties reported by Yildiz et al. (2009) for wild Turkish chestnuts 19

Table 5. Air Flow Separator testing data. 27

Table 6. Dowel Grid Separator testing data. 30

Table 7. Axial-Dowel Wheel Separator testing data. 33

Table 8. Radial-Dowel Wheel Separator testing data. 36

Table 9. Deflection Separator testing data. 38

Table 10. Momentum Transfer Separator testing data. 40

Table 11. Independent Variables and their levels 45

Table 12. Testing data for chestnut loss and separation efficiency as a percentage 48

Table 13. Analysis of variance table for chestnut loss data 49

Table 14. Analysis of variance table for separation efficiency data 52

Table 15. Linear regression analysis for chestnut loss based on the number of chestnuts and feed rate 56

Table B.16. Air Flow Separator air velocities. 64

Table B.17. Dowel Grid Separator air velocities. 72

Table B.18. Axial-Dowel Wheel Separator air velocities. 75

Table B.19. Momentum Transfer Separator air velocity measurements. 81

List of Figures

Figure 1. $7,000 machine pay off prediction point for 3000 lbs/acre. 7

Figure 2. $40,000 machine pay off prediction point for 3000 lbs/acre. 8

Figure 3. Solids velocity for various air velocities as geometric diameter increases 11

Figure 4. Reproduced from Srivastava et. al. 2006, "A pneumatic conveying state diagram"..... 12

Figure 5. Material flow and characteristics inside of a conveying duct. 13

Figure 6. Cyclone separation systems: (a) depositing chamber (b) depositing chamber with cross current flow 16

Figure 7. A component view of the harvesting platform showing: (1) trailer, (2) engine, (3) Fan/Blower, (4) Saltation Sieve Separator, (5) flexible harvest tube and nozzle; (6) fan/blower discharge; (7) fan inlet. 21

Figure 8. The harvesting platform. 22

Figure 9. Air Flow Separator and regions: (a) conveying region, (b) deposit chamber, (c) inlet. 26

Figure 10. Air Flow Separator 26

Figure 11. Dowel Grid Separator and regions: (a) conveying region (CR), (b) deposit chamber (DC), (c) inlet. 28

Figure 12. Dowel Grid Separator 29

Figure 13. Dowel Grid Separator conveying regions 1, 2, and 3. 29

Figure 14. Clogging in the conveying region of the Dowel Grid Separator. 31

Figure 15. Axial-Dowel Wheel Separator: (a) conveying region, (b) deposit chamber, (c) rotating dowel cylinder, (d) deflection plate. 32

Figure 16. Axial-Wheel Separator. 32

Figure 17. Conveying region of the Axial-Dowel Wheel Separator, with components: (a) dowel rod rotating cylinder and (b) deflection plate. 33

Figure 18. Radial-Dowel Wheel Separator: (a) conveying region, (b) deposit chamber, (c) inlet. 35

Figure 19. Radial-Dowel Wheel Separator conveying region and (a) slotted inlet plane, (b) dowel rod spindle, (c) deflection plate and (d) self cleaning apparatus. 35

Figure 20. Deflection Separator: (a) conveying region, (b) deposit chamber and (c) inlet. 37

Figure 21. Deflection Separator conveying region with (a) dowel rods and (b) deflectors.......... 38

Figure 22. Momentum Transfer Separator: (a) momentum skids, (b) separation grid, (c) deflection point. 40

Figure 23. Saltation Sieve Separator conveying region. 42

Figure 24. Saltation Sieve Separator (SSS). 43

Figure 25. Saltation Sieve Separator components: (a) momentum skids, (b) hinged paddle, (c) conveying region, and (d) deposit chamber. 44

Figure 26. Chestnut loss percentage as affected by the number of chestnuts (Ch) and weight of debris (D). 49

Figure 27. Chestnut loss as affected by the number of chestnuts (Ch) and the feed rate (FR)..... 50

Figure 28. Chestnut loss as affected by weight of debris (D) and feed rate (FR)........................ 51

Figure 29. Response surfaces for separation efficiency as affected by number of chestnuts (Ch) and weight of debris (D). 53

Figure 30. Separation efficiency as affected by the number of chestnuts (Ch) and feed rate (FR). 54

Figure 31. Separation efficiency as affected by weight of debris (D) and feed rate (FR). 55

Figure B.32. Velocity measurement positions in the Air Flow Separator. 63

Figure B.33. Air Flow Separator air velocities at position 1. 65

Figure B.34. Air Flow Separator air velocities at position 2. 66

Figure B.35. Air Flow Separator air velocities at position 3. 67

Figure B.36. Air Flow Separator air velocities at position 4. 68

Figure B.37. Dowel Grid Separator air velocity measurement positions. 69

Figure B.38. Dowel Grid Separator air velocities at position 1.. 70

Figure B.39. Dowel Grid Separator air velocities at position 2.. 71

Figure B.40. Air Flow Separator air velocities at position 3. 72

Figure B.41. Axial-Dowel Wheel Separator air velocity measurement positions. 73

Figure B.42. Axial-Dowel Wheel Separator air velocities at position 1. 74

Figure B.43. Axial-Dowel Wheel Separator air velocities at position 2. 75

Figure B.44. SSS air velocity measurement positions... 76

Figure B.45. SSS velocity profile at position 1. 77

Figure B.46. SSS velocity profile at position 2. 78

Figure B.47. SSS velocity profile at position 3. 79

Figure B.48. SSS velocity profile at position 4. 80

1 Introduction

In the past five years, chestnut (*Castanea sp.*) production in the United States has risen to the highest levels since the early twentieth century. In 2007, the United States Department of Agriculture (USDA) census lists 1200 chestnut farms totaling 3,335 acres of chestnuts; Michigan chestnut growers account for twenty four percent, or 813 acres, of the total chestnut acres in the US (United States Department of Agriculture: Census of Agriculture 2007). Forty percent of these acres reported are non-bearing age. With the increase in chestnut production, and rising labor costs associated with harvesting, an economical harvesting machine is desired.

Chestnuts grow in a protective shell, called a bur, and ripen on the tree during a summer growing season. They are harvested from the orchard floor after they mature and fall to the ground. Mature chestnuts either leave the bur completely or are partially contained inside the bur. During harvest, orchard debris is additionally collected and harvested material typically includes chestnuts, chestnuts partially in burs, chestnuts completely in burs, empty burs, and foreign materials such as leaves, twigs, dirt/stones, and grass. Decisions on whether a bur encased chestnut lying on the orchard floor is “good”, is subjective amongst Michigan chestnut growers. Some growers consider these nuts to be immature and can be discarded. Others prefer to retain these chestnuts.

Michigan chestnut growers need a reliable and cost effective method to harvest chestnuts from their orchards. For most Michigan chestnut growers, current machines are unaffordable based solely upon their chestnut yield. The average size chestnut orchard in Michigan is 5 acres; the average size US orchard is less than 3 acres. Worldwide, chestnuts are typically harvested by one of the following methods: 1) hand harvesting with hand held tools or gloves, 2) mechanical sweeping, or 3) mechanical sweeping and vacuum combination.

2 Literature Review

Literature for harvesting chestnuts was not found in any published articles; however, vacuuming systems are widely used throughout the agricultural industry. Coates and Lorenzen (1990) successfully designed and built two vacuum harvesting machines for jojoba seeds. Although the jojoba seed is smaller than the chestnut, the machine functionality can be considered for chestnuts. Their harvesting system consisted of vacuuming heads traveling above the ground, beneath the jojoba bushes. Harvested material is moved through a high velocity air stream which separates material based on density. Seeds and other material fall to the bottom of the separation chamber and exit through an airlock system. A positive pressure air system conveys the seeds to a seed hopper for short term storage. Their conclusions are: a vacuum head system of this type sufficiently collects seed from the ground, harvesting efficiency varied with field conditions, and an automatic lateral control parameter was needed for the head design. They replaced fan blades multiple times during harvest due to excessive wear from sand, dirt, and rocks traveling through the fan. Finally, they recommend improving the air-cleaning system as they deemed theirs "inadequate".

Chestnut harvesting machines typically windrow material into a ground collection system. Ground collection systems have two primary functions: material engagement and delivery control. A common mechanical ground collection system uses fingers or paddles made of rubber, to lift material from the ground. The material is then offloaded onto a conveyor, which is typically slotted, holed, or made of rollers and chains. Cross flow air systems are used to pneumatically sort lighter debris from the desired product. Vacuum ground collection systems use negative air pressure and aerodynamic drag to lift material from the ground, through a nozzle and hose. The harvested material is then conveyed through flexible tubing to the main processing system of the machine. In some cases, these processing systems include a series of mechanical scuffing devices which loosen chestnuts from debris.

FACMA, an Italian agricultural equipment manufacturer, has developed a machine currently being used for harvesting chestnuts, hazelnuts, almonds, walnuts, coffee beans, macadamia nuts, and olives. This machine consists of two rotating paddle disks in front of the machine which windrow orchard material into a vacuum collection tube. The harvested material is collected in an airlock sorting chamber. Material entering the airlock chamber encounters a rigid mounted rubber baffle which drops the material to the air lock system, and prevents material from entering the fan inlet. The material leaves the chamber, via an air lock paddle, where it is dropped over an air stream. The material not separated is moved to a dual rotational drum sieve for separation and shucking. A second air stream separates debris loosened in the drum sieve and places it on the orchard floor. A positive pressure system is used to transport chestnuts to a bagging station at the rear of the machine.

Compared to the current mechanical and vacuum harvesting systems, a single-stage vacuum harvesting system has potential. Negative air pressure can be used to pick-up and convey debris, and eliminate the need for a mechanical ground collection system. Because the air is the product carrier, the need for additional components such as belts and chains is minimized.

3 Objective

The overall objective of the research was to design a single-stage vacuuming technique to harvest chestnuts and sort field debris, and analyze the system performance based on chestnut loss and separation efficiency.

Michigan's chestnut growers, and similarly sized producers, currently rely on hand labor as the most economical form to harvest their chestnuts. These labor wages for harvest and handling procedures are increasing resulting in higher operational costs. The availability of labor is also decreasing and often hard to find. In order to help Michigan chestnut growers progress and remain profitable, farm level harvesting economics must be addressed. The first objective for this research is:

1. Define an economic affordability range for purchasing a harvesting machine, strictly related to chestnut yield and orchard size.

A simple economic model can be used to predict a point in which purchasing a machine can be more economic than paying labor wages for harvesting. Harvesting duration, labor wages and pick up rates, along with machine costs impact this prediction point.

2. Design a single stage vacuuming system to harvest chestnuts and sort field debris.

Because costs associated with machinery depend largely on complexity, a single-stage system is highly desirable. A single-stage system decreases the number of components; potentially making a harvesting machine more economical for Michigan growers.

3. Evaluate the harvesting technique using two performance parameters: chestnut loss and separation efficiency.

A vacuum harvester can be designed to harvest chestnuts using a single-stage separation technique. The technique will sort field debris from chestnuts while minimizing chestnut loss. The system needs to be a viable economic option for Michigan, and similar sized, chestnut orchards.

4 Justification

In order to help developing chestnut growers progress and remain profitable, farm-level harvesting economics were addressed. The economic model developed for a chestnut harvesting was used to predict a point where purchasing and operating a harvesting machine is more economical than hiring manual labor, based on varying parameters. The average sized chestnut orchard in Michigan is 5 acres and less than 3 acres for the United States.

Harvesting chestnuts is a value-added process for Michigan growers and the economic benefits are substantial for growers with smaller orchards. For example, purchasing an efficient $7000 harvesting machine can be more economical than paying labor wages when a grower has 2 1/2 acres producing 2000 lbs/acre (based on economic model below). An in-orchard harvest and separation process can lower a grower's cost associated with less efficient manual harvesting and sorting. Chestnuts are typically harvested every two days, resulting in a high demand for labor followed by an idle period. A harvesting machine can potentially reduce the peak labor demand.

The economics of a vacuum harvester were calculated using procedures given by Srivastava et al. (2006) and Bainer, Kepner and Barger (1955). For this analysis, the following assumptions were used, and based on current economic values and information provided from Michigan chestnut growers. These assumptions are:

1) Machine annual fixed costs are 15% of the purchase price.

2) An acre yield is 3000lbs.

3) A person can harvest 38lbs/hr.

4) A person is paid $8/hr.

5) The harvest season is 21 days.

6) A day consists of 8hrs of harvest time.

7) The initial cost of a machine is $7,000.00.

8) Repairs are necessary.

9) Annual usage is 150 hrs/yr.

10) A harvesting machine can harvest 6 acres in one day.

11) Machine function is limited to 12 acres.

The model used to predict an economic point for purchasing a machine is described below:

Machine

$$Annual\ Fixed\ Cost\ [\$] = 0.15 * Purchase\ Price\ (\$) \tag{1}$$

$$Annual\ Variable\ Cost\ [\$] = \left(\$4.25 + Wage\ (\frac{\$}{hr})\right) * Annual\ Usage(hr) \tag{2}$$

$$Total\ Machine\ Cost\ [\$] = Annual\ Fixed\ Cost + Annual\ Variable\ Cost \tag{3}$$

Labor

$$AnnualWages[\frac{\$}{acre}] = \frac{Yield(lbs/acre)}{PickupRate(lbs/hr)} * Wage(\$/hr) \quad (4)$$

Figure 1 depicts the intersection point, or acreage needed to economically purchase a $7,000 machine based on 3000 lb/ac yield and a manual labor pickup rate of 38 lbs/hr. The acreage needed was approximated at 2 acres. Decreasing the orchard yield will increase the acreage needed to economically afford the same machine, based on the same assumptions.

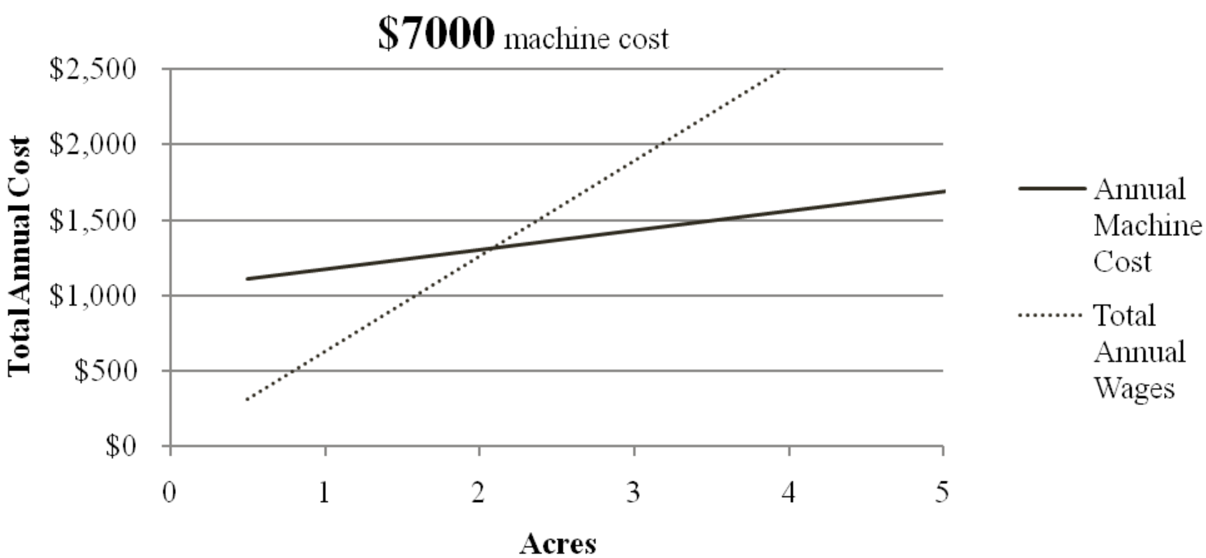

Figure 1. $7,000 machine pay off prediction point for 3000 lbs/acre.

When the purchase price of the machine was increased to $40,000 the acreage needed to purchase a harvesting machine was approximated at 12 acres as shown in Figure 2. This assumes a yield of 3000 lbs/ac and a manual labor pick up rate of 38 lbs/hr.

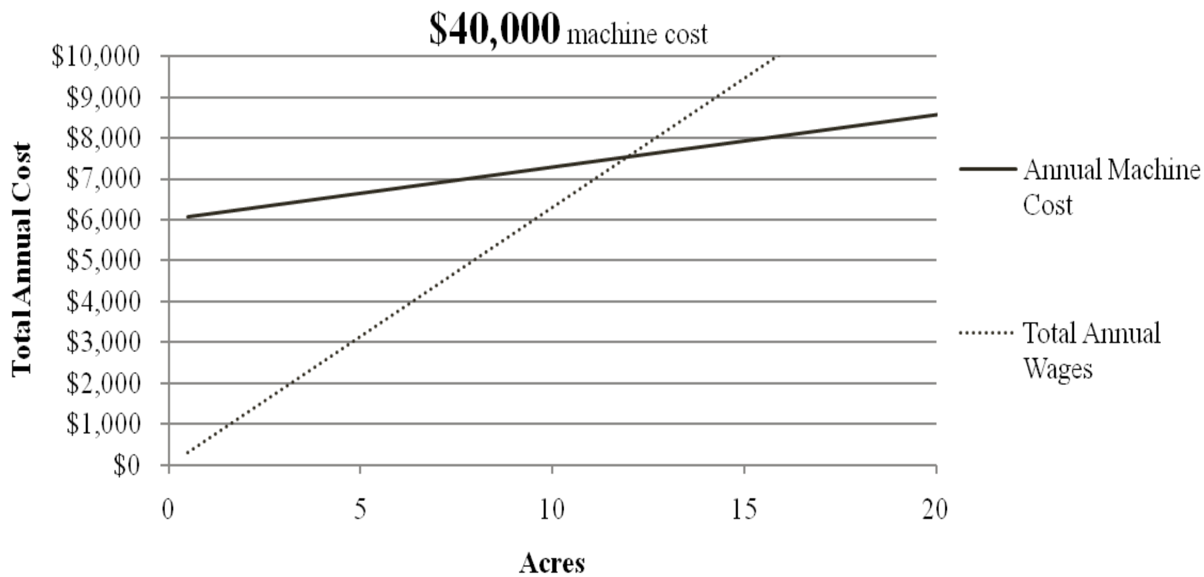

Figure 2. $40,000 machine pay off prediction point for 3000 lbs/acre.

Due to the size of Michigan chestnut orchards (~5ac) yield is an important factor in determining economics. Various yields were evaluated using the economic model to account for typical orchard yields in Michigan. Table 1 shows yield comparison with varying machine purchase price. A harvesting machine which is economically feasible for a producer of average 2-12 acres is not known to exist. This is the target range for the economic justification.

A chestnut grower producing 1500 lbs per acre, on 4 acres, could purchase a $5,000.00 harvesting machine. That same grower would need approximately 33 acres to offset a $40,000.00 machine, which are currently commercially available. The productivity of labor work influences the break-even point and should be considered.

Table 1. Acreage estimated to economically afford a harvesting machine at various yields. For interpretation of the references to color in this, and all other figures, the reader is referred to the electronic version of this thesis.

Yield (lb/acre)	Assumed Purchase Price of a Machine ($)				
	$2,000.00	$5,000.00	$7,000.00	$15,000.00	$40,000.00
500	none	none	none	none	none
1000	~ 6.5	~ 10	~ 15	~ 29	> 50
1500	~ 1.5	~ 4	~ 6	~ 12	~ 33
2000	~ 1.5	~ 3	~ 3	~ 8	~ 21
2500	< 1	~ 2	~ 2.5	~ 6	~ 16
3000	~ 0.5	~ 1.5	~ 2	~ 5	~ 12

When a grower's yield is 500lbs or less, hand labor is the most economic way to harvest, based on this model. The target acreage for this model was less than 12 acres, which is common for Michigan orchards. Predictions above this acreage need more emphasis on machine capacity and if numerous machines would be needed. Grey cells in Table 1 are outside of the range of this economic model and need reconsideration.

5 Design Process

5.1 Separation Concepts and Strategies

A vacuuming system was initially decided upon based on achieving our criteria for a single-stage system. The design of this type of system is based on horizontal and vertical pneumatic conveying of materials. Research has proven useful and these conveying systems are used in various industries, including agriculture. Some advantages of pneumatic conveying are: flexibility of routing from horizontal to vertical, multiple distribution locations, generally low maintenance, and ease of user control. Some disadvantages are: high power consumption, wearing of fan components due to material discharge, limited distance of conveyance, and the complexity and unpredictable nature of fluid flow.

Vertical conveyance depends upon the terminal velocity of the chestnut. Terminal velocity is defined as the force required to overcome gravitational and drag forces acting on an object. It should be noted that the terminal velocity is not adequate for transport; rather it is a quantitative description useful for initial design and fluidization of a particle. To suspend or fluidize a chestnut in a vertical conveyance region, the air velocity should never be less than the terminal velocity. A relationship exists between the air velocity and solids velocity which contains a geometry variable, shown in equation 5. This relationship was used to design geometry specific to sorting by density.

Marcus et al. (1990) reported an equation estimating the solids velocity (c):

$$\frac{c}{v} = 1 - 0.68 d^{0.92} \rho_p^{0.5} \rho_a^{-0.2} D^{-0.54} \qquad (5)$$

Where:

c = solids velocity, m/s

v = velocity of air, m/s

ρ_a = density of air, kg/m^3

ρ_p = density of particles, kg/m^3

d = particle mean diameter, m

D = diameter of conveying tube, m

MATLAB was used to calculate and plot the velocity for solids as shown in Figure 3. The diameter of the conveying tube was varied from 1 to 36 in. (0.0254 to 0.9 m). Diameters over 36 in. (1 m) where considered too large for this scale system.

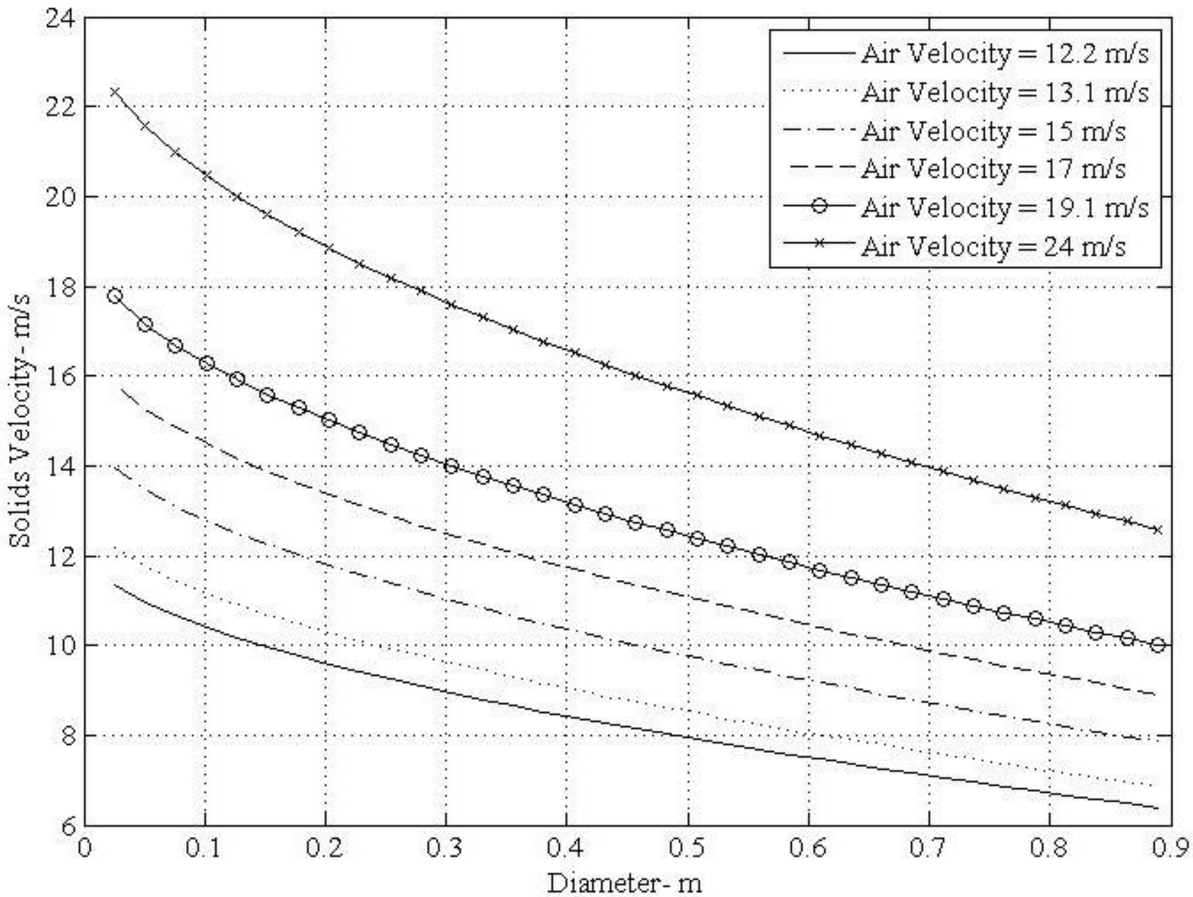

Figure 3. Solids velocity for various air velocities as geometric diameter increases

A distinguishable relationship exists between the terminal velocity and saltation velocity. Chestnuts entering an air stream are subjected to aerodynamic drag effectively determining the pick-up capability. The saltation velocity, or critical air velocity required for horizontal conveyance, has been published for several agricultural commodities. Figure 4 shows a graph of superficial air flow versus pressure drop per unit length. The inflection point separates the two flow phases, dense and dilute. This inflection point was used to predict velocities required to keep chestnuts in the dilute phase.

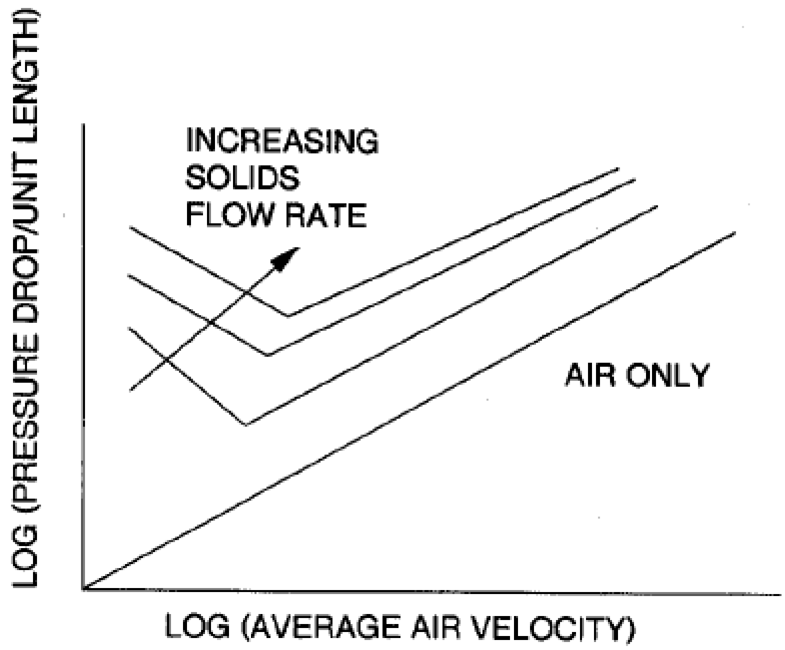

Figure 4. Reproduced from Srivastava et. al. 2006, "A pneumatic conveying state diagram".

Horizontal conveyance is classified in three phases: dilute phase, dense phase, and fixed bed. Dilute phase refers to fully suspended particles moving separately through a conveyor pipe; this occurs when the air velocity is much greater than the minimum saltation velocity for that particular particle. Fixed bed formation is considered as material not moving, or settling, in the conveyor pipe; this occurs when the air velocity drops below the minimum saltation velocity needed. Dense phase conveyance refers to the in-between. In horizontal conveyance, material generally bounces along the bottom of a duct. The distance between a bounce or wall interaction is random and hard to predict, especially with non-uniform chestnut shape. Tilting a conveying duct will increase the chestnut interaction with the wall, as depicted in Figure 5. Less air flow results in dense phase conveyance, leading to bed formation.

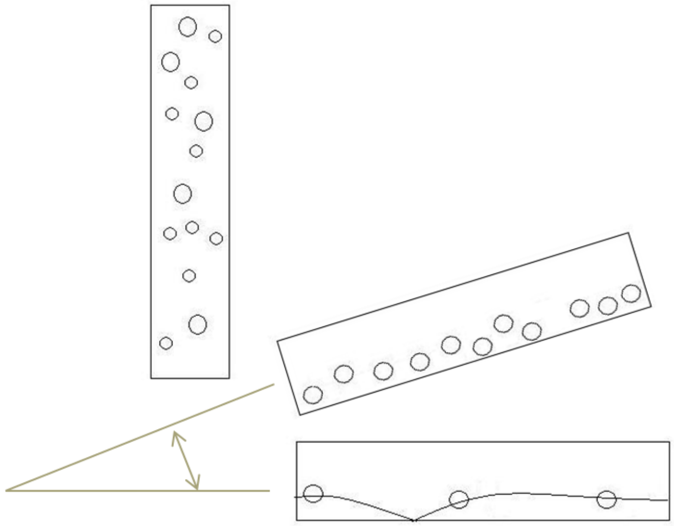

Figure 5 Material flow and characteristics inside of a conveying duct.

Marcus et al. (1990) developed a table relating air velocities for horizontal and vertical transport. They stated that in the case of fine particles, the horizontal conveying velocity ranges from 3 to 5 times larger than vertical conveying velocities. They also state that the difference in conveying velocities is much smaller for coarser particles. The velocities for various agricultural products are shown in Table 2 (Marcus et al. 1990).

Table 2. Reproduced from Marcus et al. 1990.

Material	Bulk density (kg/m^3)	Vertical Conveyance Velocity (m/s)	Horizontal Conveyance Velocity (m/s)
Alum	800	19.8	33.5
Calcium carbonate	440	19.8	33.5
Coffee beans	672	13.7	22.9
Hydrated lime	480	12.2	27.4
Malt	449	16.8	30.5
Oats	400	16.8	30.5
Salt	1440	25.3	36.6
Starch	640	16.8	27.4
Sugar	800	18.3	33.5
Wheat	769	16.8	32

5.1.1 Fluidized Beds

A fluidized chamber design was initially considered as one potential method for separating chestnuts from debris. Using an upward directed fluid passing through harvested material was tried by Guyer and Kang (2009), in efforts to fluidized lighter particles. Fluidized beds can be described as the Winkler process from the 1930's, or gas solid fluidization (Douglas and Walsh, 1966). Coal is typically fluidized to separate undesirable materials or minerals before entering a combustion process. Fluidized beds have been used to sort agricultural products spanning back 100 years or more.

The fluidization process allows separation to take place according to varying densities. Zaltzman et al. (1983) studied and tested fluidized bed mediums as a separation process. An analytical model was developed for this separation process (Zaltzman 1986) based on gravitational motion of a sphere in a fluidized bed, which was tested in a laboratory by Mizrach et al. (1984). Further work was conducted for separating flower bulbs from stones and clods using the fluidization process (Zaltzman et al. 1985). Zaltzman and Schmilovitch (1986) leveraged this process for sorting potatoes from stones and clods. Research expanded into other agricultural commodities investigating the separation potential related with density and quality. The relationship between density and quality has been observed in potatoes, tomatoes, peaches, peas, pecans, citrus fruits, watermelons, and small seed and grains (Zaltzman et al. 1987). They concluded that quality changes due to maturity or quality can generally be associated with a change in density.

From the previous research studies, sorting chestnuts from debris based on density characteristics seems feasible. Although density associated with chestnut fruit quality has not been published, Michigan growers routinely dip harvested chestnuts in a water bath and scoop away the "floaters". This processing practice leans toward Zaltzman's observations and general predictions associated with other agricultural commodities.

5.1.2 Cyclone Separation Systems

Agriculture has employed the use of cyclone separation systems along with material processing industries, product handling industries and food industries. Cyclone separation systems are widely studied and are extremely efficient. These systems separate material from an air stream by exerting forces on the material. Typically the air stream enters a cylinder at a tangential point in the sidewall. Gravitational forces, inertia forces, and friction, contribute to the effectiveness of a cyclone separation system.

Cyclone separation chambers used for sorting include two basic types: depositing chamber, and depositing chamber with cross-current flow. Inlets vary from tangential, spiral, and axial entrances. Each system is designed according to a specific need. The depositing chambers separate materials based on their densities and differing velocities. For a standard depositing chamber, the air velocity drops due to a diameter increase and gravitational forces acting on the material become influential. The heavier material tends to drop from the air stream first. Figure 6 represents a depositing chamber and a depositing chamber with cross current flow.

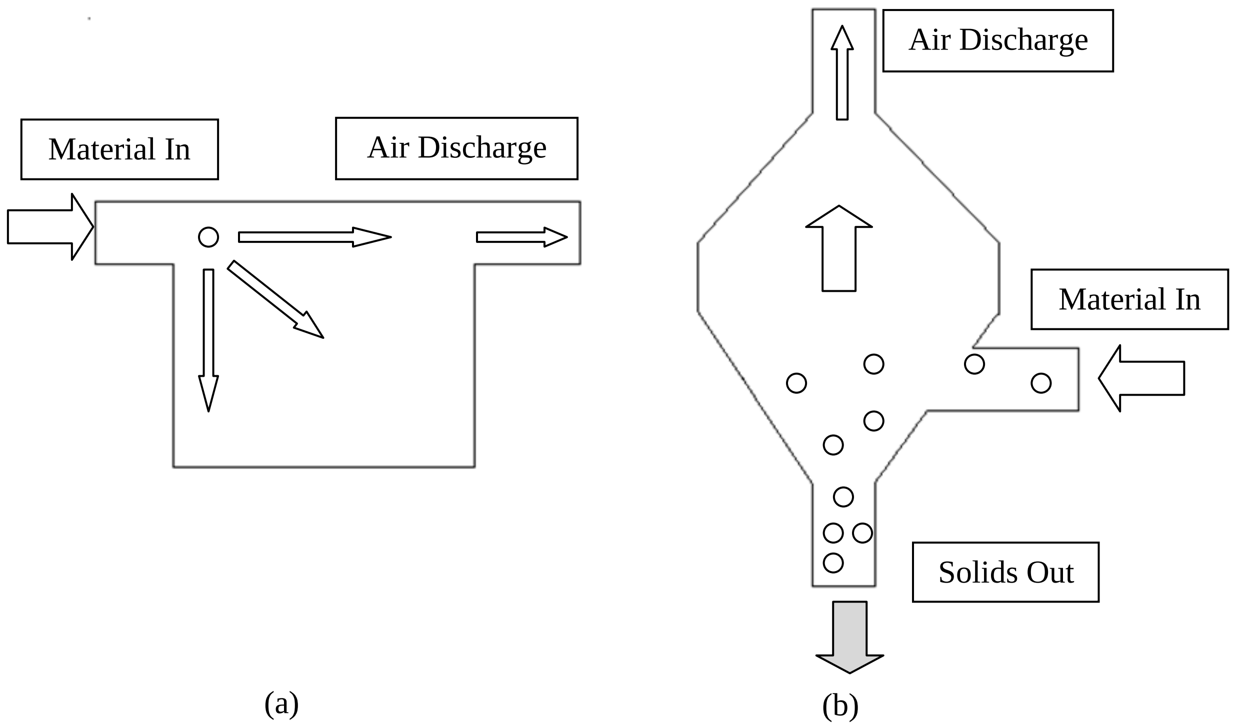

Figure 6. Cyclone separation systems: (a) depositing chamber (b) depositing chamber with cross current flow

A depositing chamber with cross current flow closely resembles the initial design consideration for this research. Air flow enters the depositing chamber from the bottom and exits through the top, carrying lighter material and debris. A single-stage vacuuming system allows for this type of design but mass flow must be taken into consideration. Drawing air from two places increases the pressure drop across each path, requiring additional horsepower to maintain sufficient air velocity at the suction nozzle.

In equilibrium state, the forces on a particle are the aerodynamic or drag force and the weight of the particle minus the air lifting force (Marcus et al. 1990). This assumption holds true for a spherical shape. Theoretically, a chestnut was assumed to be spherical for calculations. Marcus et al. (1990) provide the following force balance representation:

$$F_D = F_G - F_{lift} \qquad (6)$$

$$F_D = C_D A \frac{\rho}{2} w_f^{\,2} \qquad (7)$$

Where:

F_D = drag force

F_G = gravitational force

F_{lift} = lifting force

C_D = drag coefficient

A = area of sphere

ρ = density of air

w_f = settling velocity

For a cross current separation chamber the separation efficiency depends upon the settling velocity. Marcus et al. (1990) calculated the theoretical efficiency of three different sized separator diameters: 3m, 6m, 25m. The efficiency of separation decreased as diameter increased due to geometry and the forces acting upon a particle inside of a depositing chamber. This research builds upon these principles and applies them specifically to harvesting chestnuts in Michigan.

5.1.3 Physical Properties of Chestnuts and Burs

Guyer and Kang (2009) reported the following air velocities related to chestnuts, chestnuts in burs, and burs, shown in Table 3. The air velocity required to pick up chestnuts was reported as 19.3 m/s. From Figure 3, the 19.3 m/s air velocity plot yields a solids velocity of approximately 15 m/s, in a 8 inch tube. This velocity agrees with the terminal velocity of Turkish chestnuts, reported in Table 4.. The difference can be attributed to the particle or geometric mean diameter between the chestnut species being tested.

Table 3. Air velocities sufficient for vacuuming chestnuts, chestnuts in burs, and burs. Reproduced from Guyer and Kang (2009)

Material	Weight (g)	Length (mm)	Width (mm)	Thickness (mm)	M.C. (%,w.b.)	Suction Pressure (mm,wg)	Air Velocity (m/s)
Empty burs	6.06	78.56	48.76	34.1	10.73	82	12.2
	8.86	77.91	79.19	54.64	10.61	82	12.2
	21.16	73.68	71.86	33.31	63.56	104	13.1
	46.24	82.26	79.76	59.96	73.68	104	13.1
	49.49	91.17	84.42	74.84	68.11	104	13.1
Burs with Nuts	13.3	64.37	63.73	51.53	32.11	104	13.1
	25.23	66.34	59.67	47.7	66.71	104	13.1
	39.46	65.54	64.21	59.8	57.2	104	13.1
Nuts	7.24	33.83	32.39	18.93	15.88	129	19.3
	8.49	33.95	30.59	17.07	42.29	129	19.3
	13.54	35.2	33.47	23.68	46.6	129	19.3

Yildiz et al. (2009) reported physical properties of wild chestnuts grown in Turkey. Included in their analysis is terminal velocity for chestnuts, bulk densities, and geometric averages. Table 4 is reproduced from a collection of tables by Yildiz.

Table 4. Physical properties reported by Yildiz et al. (2009) for wild Turkish chestnuts

Turkish Chestnut Properties at 51.32% m.c.d.b.	
Length (mm)	21.79
Weight (mm)	23.94
Thickness (mm)	14.55
Geometric mean diameter (mm)	19.62
Sphericity	0.889
Bulk Density (kg/m3)	585
Terminal Velocity (m/s)	14.51

Two varieties of chestnuts were used in this study: Colossal and Chinese. Both varieties differ from the wild Turkish chestnuts in all categories listed in Table 4. Colossal chestnuts are generally larger with more mass and Chinese chestnuts are smaller than both the wild Turkish chestnuts and Colossal. Michigan chestnut growers have several varieties currently planted; although the majority of chestnuts produced are either Colossal or Chinese.

Chestnuts were assumed to be round for computational purposes but typically chestnuts are flat on one side; the actual projected area of a chestnut in the air stream can be rectangular and significantly smaller than a chestnut's spherical projected surface area. A chestnut's obscure shape has a different saltation velocity than a round chestnut and will vary, depending on the size and shape of the chestnut. As the size of chestnuts increase the difference between the terminal velocity and saltation velocity decreases. Smaller chestnuts will have a larger saltation velocity than larger chestnuts.

5.2 Machine Design

Saltation velocity for wheat was determined through experiments conducted by Shen, Haque, Posner (1994). They used stepwise regression to formulate the best multi variable regression equation. The equation provided a R^2 value of 0.974.

$$V = 22.70 + 2.01 * m.c. + 3.61 * Q - 1.19 * 10^{-3} * (d_p * m.c.) + 8.5 * 10^{-4} (A_p * T) - 0.28 * (A_p * m.c.) \quad (8)$$

Where:

V = Saltation velocity (m/s)

$m.c.$ = Moisture content (%, w.b.)

Q = Feed rate (kg/s)

d_p = Particle geometric mean diameter (m)

T = Conveying air temperature (K)

A_p = Specific surface area of the grain (cm^2/g)

Using numerical values reported by Yildiz et al. (2009) for the moisture content, particle geometric mean diameter, and specific surface area for wild Turkish chestnuts, combined with standard air temperature and an assumed feed rate of 0.15 kg/s, the saltation velocity required to keep chestnuts in the dilute phase was approximated at 4660 ft/min (23.7 m/s). Adequate conveyance velocity should not be less than the saltation velocity or drop below 4660 ft/min unless separation or bed forming is desired.

5.3 Platform

A component view of the harvesting prototype platform is shown in Figure 7. A gasoline engine (2) was used to transmit power to a fan/blower (3). The fan/blower inlet (7) was used to create the vacuum needed to pick up chestnuts. Chestnuts and debris were vacuumed from the ground and conveyed through flexible tubing (5) and through the separation device (4). Debris was expelled to the orchard floor through the blower discharge (6).

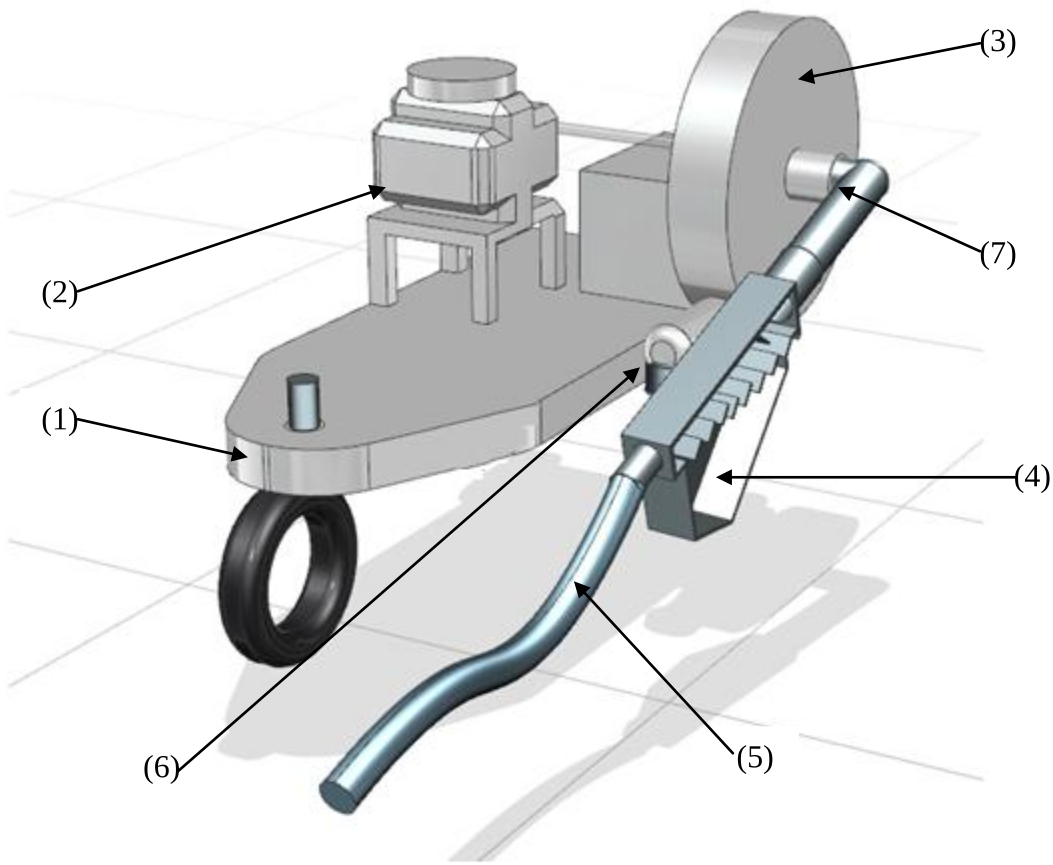

Figure 7. A component view of the harvesting platform showing: (1) trailer, (2) engine, (3) Fan/Blower, (4) Saltation Sieve Separator, (5) flexible harvest tube and nozzle; (6) fan/blower discharge; (7) fan inlet.

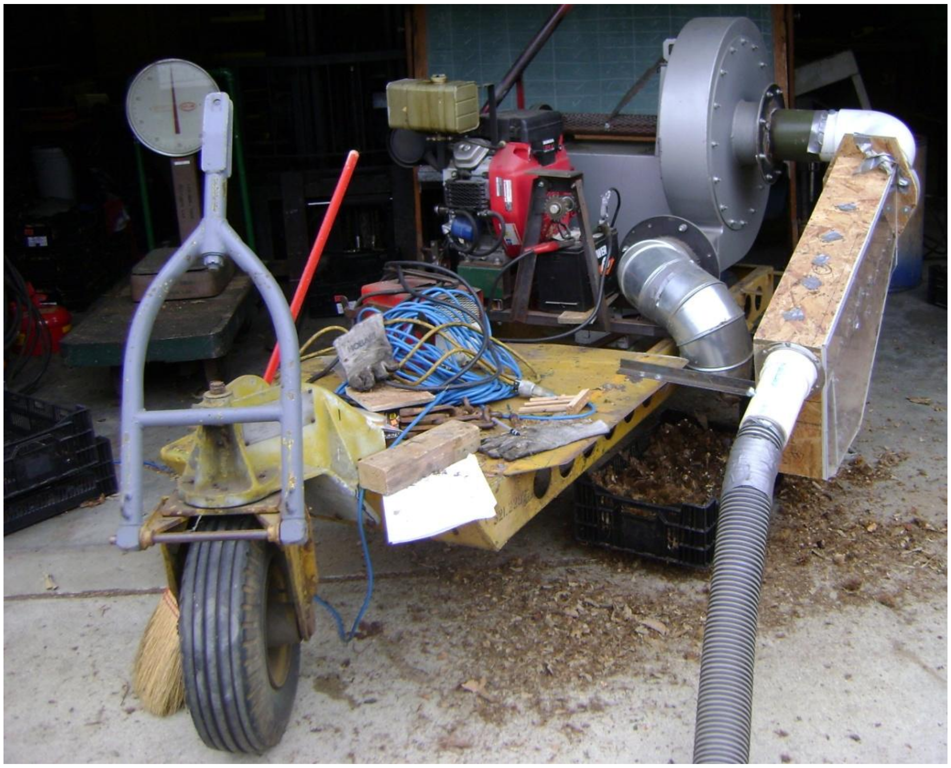

Figure 8 The harvesting platform.

5.3.1 Frame and Engine/Fan drive

A Honda GX670cc, 24.0 hp V-twin engine (http://engines.honda.com/) was used to drive a HP-8D18 high pressure radial blower, from Cincinnati Fan (http://www.cincinnatifan.com). These two components were significantly larger than necessary but were available from the department. The blower has an 18 in. wheel, 8 in. inlet and outlet flanges, and a capacity of 7000 CFM. The blower wheel was mounted to a fan shaft which was supported by two pillow block bearings. The blower base and engine were mounted to a three-wheel pull type trailer using various brackets made from angle iron. A 7 in. dual-belt drive pulley was mounted to the engine drive shaft. Twin V-belts transmit engine power to the blower drive shaft, which had a 4 in. dual drive pulley. The transmitting speed ratio is 1.75. This ratio was designed so both the engine and blower are operating in their most efficient operating range.

5.3.2 Tubing

A 22 ft., 4 in. diameter, flexible tube was used for the suction hose. A nozzle was made of a 4 in. piece of 4 in diameter, 1/4 in. steel tube, and functioned as the product engagement device. A handle, carrying strap, and suction hose support structure were fabricated to ease operation and testing comfort. The suction hose was connected to the inlet port using a 4 in. length of 4 in. diameter schedule 40 PVC pipe and a standard 4-6 in. diameter hose clamp. The sorting chamber discharge port consists of (1) 6 in. diameter schedule 40 PVC molded flange, (1) 90deg elbow, and (4ft.) 6 in. schedule 40 PVC pipe. A port adapter was fabricated to bolt on to the blower inlet, allowing the 6 in. PVC discharge pipe to fit securely inside.

5.3.3 Materials used for separation chambers

Each testing chamber was constructed from 5/8 in. particle board, having dimensions of 30 in. x 36 in. x 6 in. A 30 in. x 36 in. sheet of 3/8 in. plexiglass was used for one outer face. Standard 1 1/4 in. deck screws were used to mount the internal components and the plexiglass to the chamber base. A 4 in. PVC plumbing flange was used for the inlet of the chamber. A 6 in. schedule 60 PVC molded flange was used as the discharge port. Foam, 1/2 in., weatherproofing seal was used between the mounting faces of the SSS and the inlet, outlet, and plexiglass face.

6 Iterative Designs

Each chamber was designed to a specific hypothesis and approach for chestnut harvesting and separation, and after testing a chamber, the hypothesis was evaluated and either accepted or rejected. A rejected hypothesis was reformulated based on the knowledge and observations from the testing and applied to the design concepts for the next chamber. Listed below are the chamber designs in order of progression throughout this research project. A total of six chambers were designed and tested.

Two specific characteristics used to completely reject a hypothesis included:

1) Clogging or jamming which requires manual intervention.
2) High chestnut loss during a test.

If either of the above occurred, the chamber design was consider inadequate and the hypothesis was rejected.

6.1 Procedure

The following describes the testing procedure:

1) Set the engine rpm.
2) Record engine drive shaft and fan motor shaft rpm using a digital tachometer.
3) Lower the velometer into the chamber through drilled holes at specific, geometric, points of interest and record velocities.
4) Prepare chestnuts and materials for harvesting and record weights and number of chestnuts.
5) Begin harvesting.
6) Record weights of separation chamber material and blower discharge collection lug, and count the number of chestnuts collected.
7) Return to step 1 after adjusting the rpm (if necessary).

To measure the air stream velocity and examine the velocity profile, the velometer was lowered into the harvesting chamber. Specific geometric points of interest include: areas behind obstruction devices, at bends in the air stream, the top and bottom of the conveying region, and various locations in the sorting chamber. Measurements were taken at the closest inch intervals. Each hole was plugged after taking the velocity measurement. Air flow data and air speed corresponding to engine RPM are found in Appendix B: Velocity Profiles.

6.2 Air Flow Separator

The air flow separator design, shown in Figure 9 and 10, resembles a cyclone separation system. A direct manipulation of the conveying air stream utilizes momentum as a separation technique. Material is moved from left to right: the suction port is horizontal and the discharge port is vertical.

The hypothesis for this design is based on air velocity and physical geometric relationships. As an air stream passes through changing geometry, or orifices, the velocity of the air changes. Increasing a diameter of a hose, or geometry inside the sorting chamber, lowers the velocity of the air below the saltation velocity of chestnuts. If the velocity of the air can be lowered below the saltation velocity of the chestnuts, but not below that of debris, separation of chestnuts from debris can occur.

In order to shorten the amount of distance needed for adequate air stream separation, a bend, or redirection, was used for the incoming material. This redirects chestnuts towards an area of lesser air velocity. These chestnuts should not continue in the air stream however, lighter material should be removed.

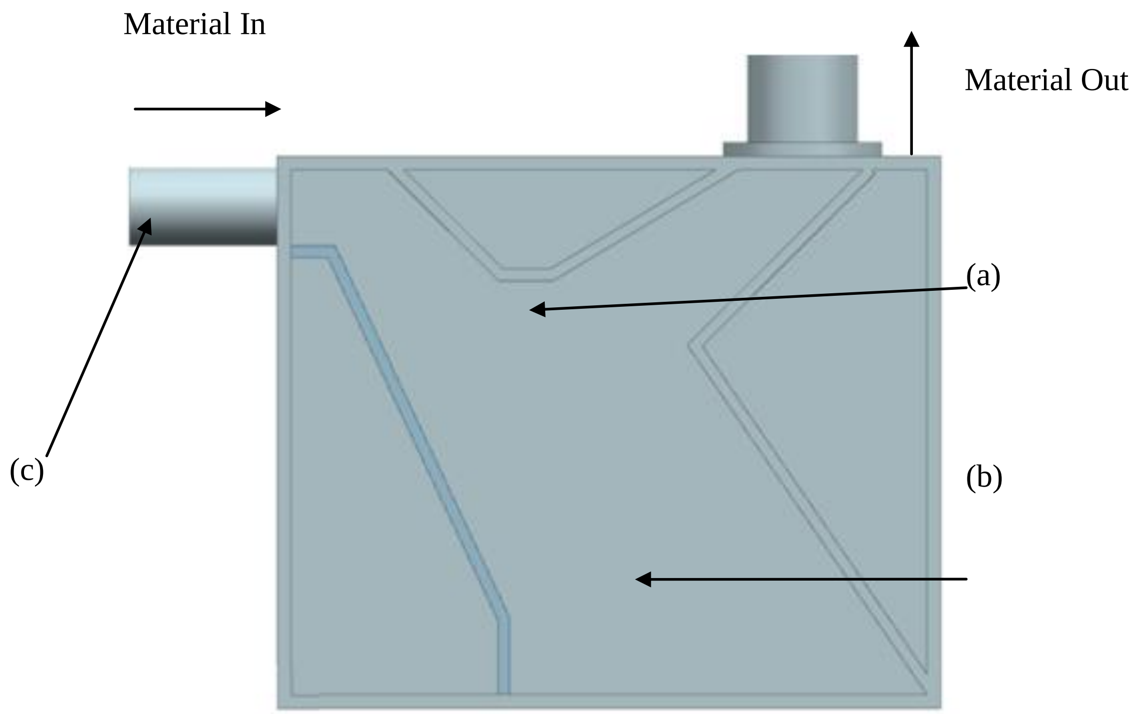

Figure 9. Air Flow Separator and regions: (a) conveying region, (b) deposit chamber, (c) inlet.

Figure 10. Air Flow Separator

Table 5. Air Flow Separator testing data.

		Material input			Collected		
	Engine RPM	Total Weight	Marked Chestnuts	Chestnut Weight	Weight	Marked Chestnuts	Discharge Weight
Air Flow Separator	1580	7lbs 10oz	50	1lb 14oz	7lb 10oz	50	0
	2580	7lbs 10oz	50	1lb 14oz	7lb 10oz	50	0
	3010	7lbs 10oz	50	1lb 14oz	7lb 10oz	50	0

Discharge weight was negligible in all three tests as shown in Table 5. Separation of material from the air stream was one hundred percent. Air flow problems are complex and air layer shrinkage was not initially considered. An observation made during the velocity profile testing shows a shrunken air layer profile specifically at the first bend inside of the chamber. The velocity of the air, at the bend, is greater in magnitude but smaller in depth. The shrunken air layer was not adequate to support debris, or chestnuts.

Engine RPM's were varied to examine the effects on the air velocity profile and performance parameters. For the Air Flow Separator, the variation in engine RPM did not have any effect on the separation performance.

Should a chestnut grower prefer no sorting, the Air Flow Separator is effective. Due to the lack of sorting, this chamber did not meet the initial objectives and the hypothesis was reformulated.

6.3 Dowel Grid Separator

The Dowel Grid Separator design consists of wooden dowel rods placed horizontally in the conveying region, as shown in Figure 11. This design exploits momentum change of the conveying material and uses a sizing grid to separate chestnuts into the deposit chamber. Figure 13 depicts the dowel rods and their respective region; dowels are spaced 1 inch apart in region 1, 1.5 inches in region 2, and 2 inches in region 3. In the y-plane of region 3, no dowel rod was within 3 inches of another. This design attempted to force chestnut burs to deflect around the dowel rod. The upward incline of dowel rods in the middle portion of the conveying region was designed to influence the flow of burs and material upward. Chestnuts should drop out of the air stream while debris will only be deflected, but still carried out of the separation chamber.

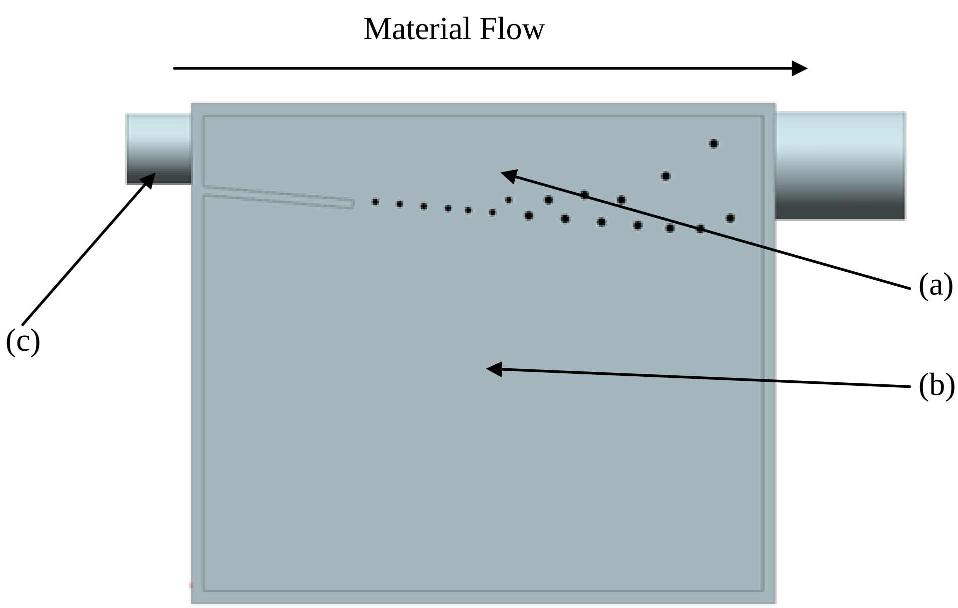

Figure 11. Dowel Grid Separator and regions: (a) conveying region (CR), (b) deposit chamber (DC), (c) inlet.

Figure 12. Dowel Grid Separator

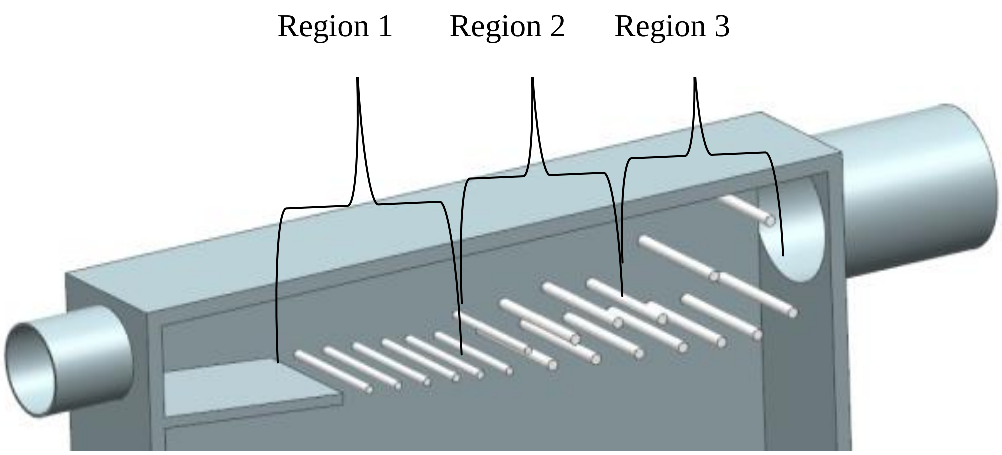

Figure 13. Dowel Grid Separator conveying regions 1, 2, and 3.

Table 6. Dowel Grid Separator testing data.

		Material In			Collected		
	Engine RPM	Total Weight	Marked Chestnuts	Chestnut Weight	Weight	Marked Chestnuts	Discharge Weight
Dowel Grid Separator	2075	7lb 8oz	50	1lb 13oz	1lb 1oz (DC) 4lb 3oz (CR)	23 (DC) 27 (CR)	2lb 4oz
	2526	7lb 6oz	50	1lb 13oz	3lb 13oz (DC) 2lb 2oz (CR)	26 (DC) 24 (CR)	1lb 7oz
	3030	7lb 8oz	50	1lb 13oz	2lb 6oz (DC) 3lb 1oz (CR)	19 (DC) 31 (CR)	2lb 1oz

Chestnut burs frequently became lodged between the dowel rods, initiating a clog as shown in Figure 14. Chestnut burs became “Velcro” like, because of their spines, in a clogging situation. The separation based on momentum change was adequate when clogging was not present. No marked chestnuts were discharged through the blower. Due to the clogging, this chamber did not meet the initial objectives and the hypothesis was reformulated.

Figure 14. Clogging in the conveying region of the Dowel Grid Separator.

Three RPM's were used to evaluate the harvesting performance for the Dowel Grid Separator. Based on the results, increasing the engine speed beyond 2075 RPM had no impact on separation. The air velocity was 3800 ft/min measured at the chamber inlet.

6.4 Axial-Dowel Wheel Separator

The Axial-Dowel Wheel Separator utilizes the horizontal dowel rod design from the Dowel Grid Separator but incorporates it into a rotating cylinder, as shown in Figure 15. The rotation of the dowel rod cylinder is done by hand when a clog starts to form. The cylinder is mounted 2.5 inches from the top of the conveying region to produce a shucking effect. A small deflection plate is mounted downstream of the cylinder to ensure no material can pass unaffected through the conveying region. An incline plane funnels chestnuts passing through the obstruction wheel back to the sorting chamber.

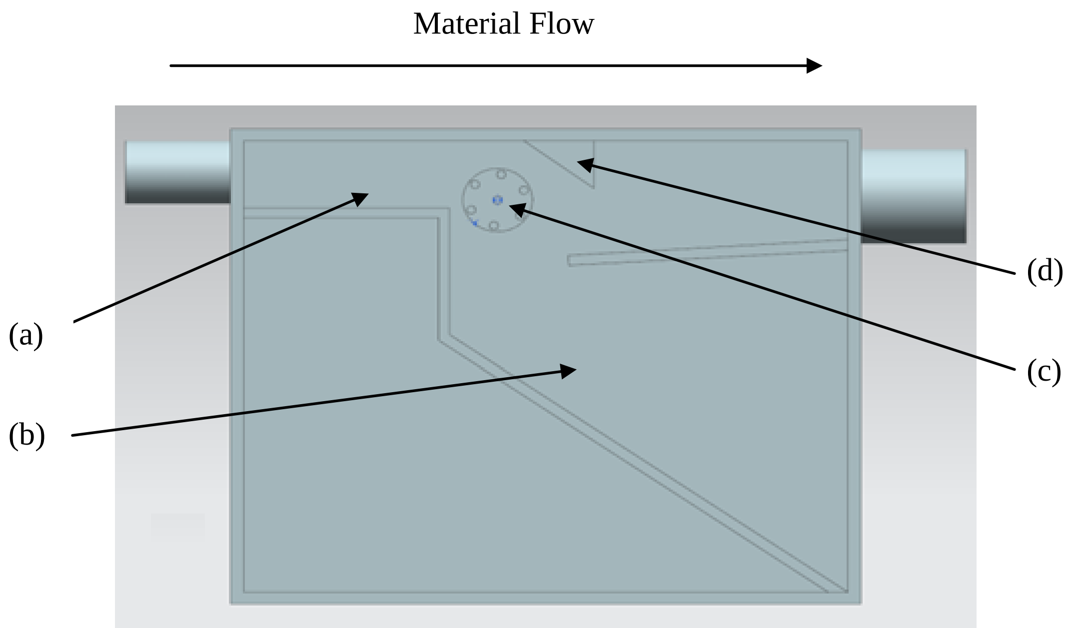

Figure 15. Axial-Dowel Wheel Separator: (a) conveying region, (b) deposit chamber, (c) rotating dowel cylinder, (d) deflection plate.

Figure 16. Axial-Wheel Separator.

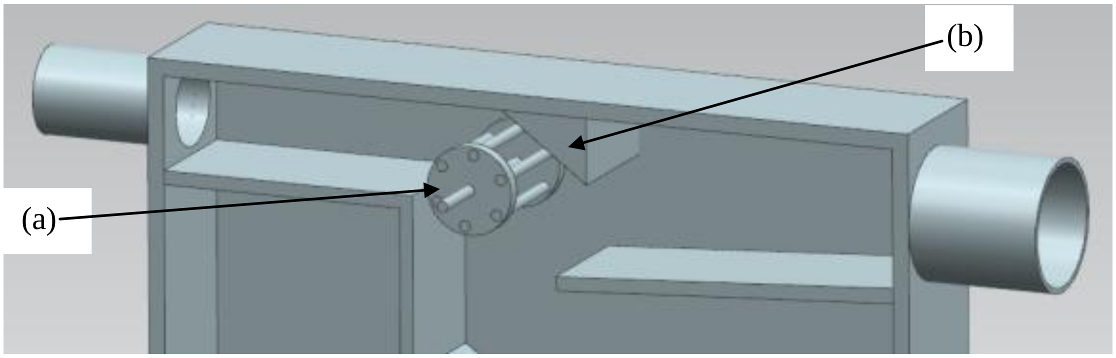

Figure 17. Conveying region of the Axial-Dowel Wheel Separator, with components: (a) dowel rod rotating cylinder and (b) deflection plate.

Table 7. Axial-Dowel Wheel Separator testing data.

		Material In			Collected		
	Engine RPM	Total Weight	Marked Chestnuts	Chestnut Weight	Weight	Marked Chestnuts	Discharge Weight
Axial-Dowel Wheel Separator	1976	8lb 10oz	50	1lb 14oz	2lb 1oz	50	6lb 8oz
	2467	8lb 10oz	50	1lb 13oz	2lb 1oz	50	6lb 2oz
	3030	8lb 7oz	50	1lb 14oz	2lb	48	6lb

Small chunks of chestnut bur became lodged between the dowel rods of the rotating cylinder. Although chestnut separation occurred, the buildup of debris over a harvesting period could produce undesirable sorting effects. A self-cleaning procedure for this type of separation system should be considered to ensure proper system functionality. Dowel rods inside of the rotating cylinder could also rotate to help facilitate self cleaning. This would require a gearing mechanism similar to a standard planetary and sun gear set-up. While this design may be suitable for harvesting and sorting chestnuts, the addition of moving components and clogging did not meet our initial requirements. The hypothesis was reformulated to address clogging.

Engine RPM's were varied to examine the effects on the air velocity profile and performance parameters. For the Axial-Dowel Wheel Separator, the variation in engine RPM did not have any effect on the separation performance.

6.5 Radial-Dowel Wheel Separator

The Radial-Dowel Wheel Separator design was to prevent clogging by using the self cleaning apparatus shown in Figure 18. Dowel rods are placed vertical in the conveying air stream and are mounted on a rotating spindle. Mounting the dowel rods vertically utilizes the momentum principles, described above, for sorting. The spacing for the spindle wheel dowel rods is one inch, which was arbitrarily selected. A second set of dowel rods is used to clean, or dislodge, any material becoming stuck between the spindle wheel dowels, as shown in Figure 19. Downward sloping planes in the conveying region funnel separated material to the sorting chamber. Slots are cut in the inlet planes to allow rolling chestnuts to pass into the deposit chamber (a), as shown in Figure 19.

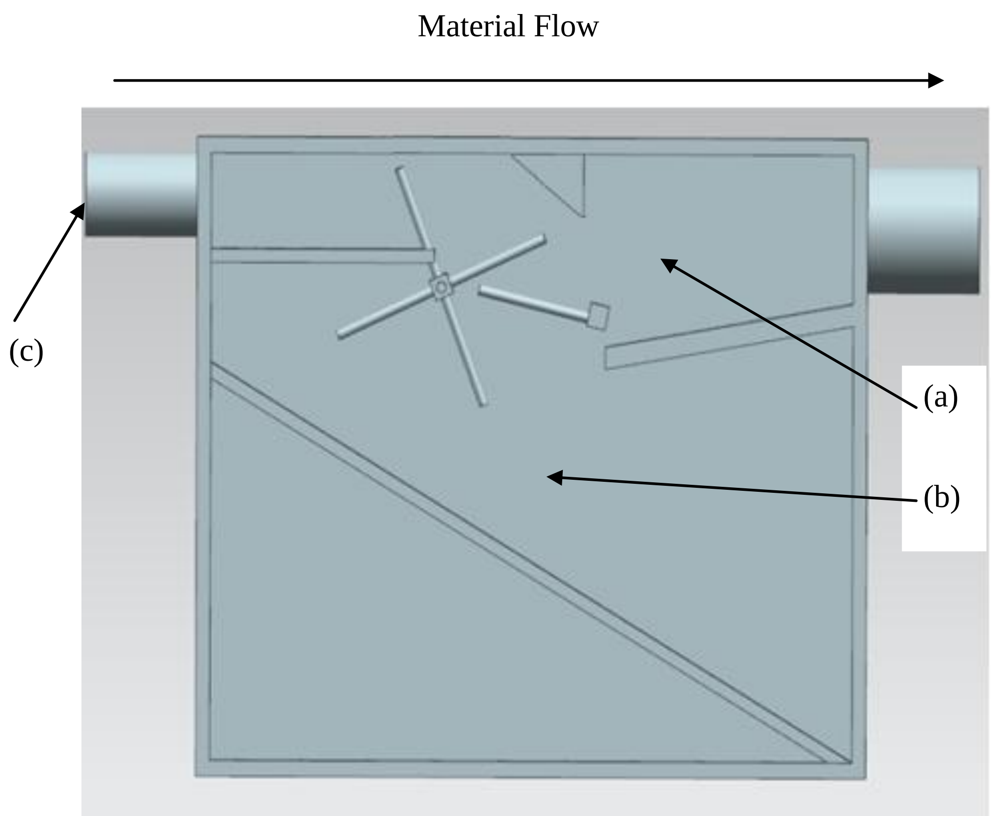

Figure 18. Radial-Dowel Wheel Separator: (a) conveying region, (b) deposit chamber, (c) inlet.

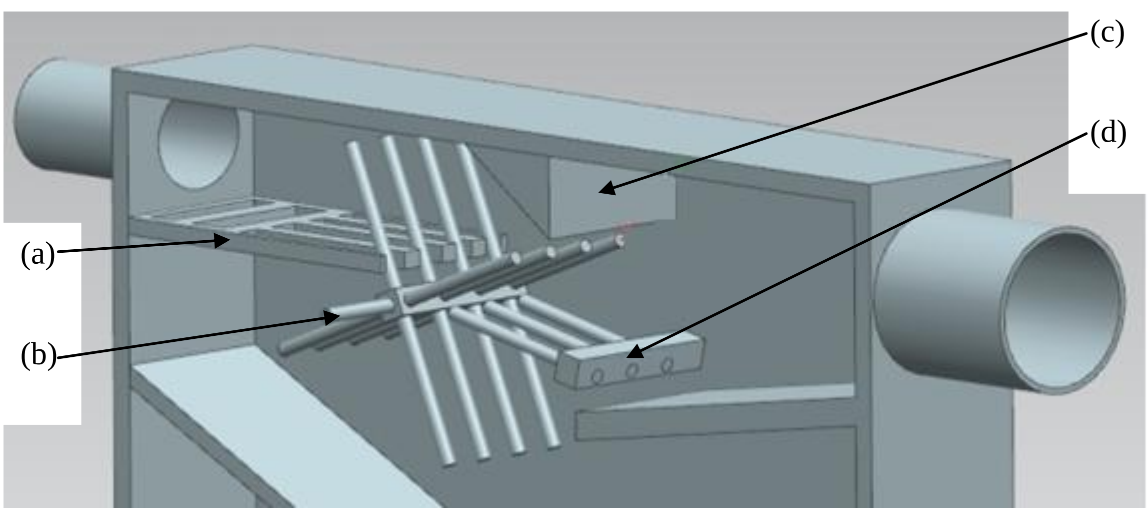

Figure 19. Radial-Dowel Wheel Separator conveying region and (a) slotted inlet plane, (b) dowel rod spindle, (c) deflection plate and (d) self cleaning apparatus.

Table 8. Radial-Dowel Wheel Separator testing data.

		Material In			Collected		
	Engine RPM	Total Weight	Marked Chestnuts	Chestnut Weight	Weight	Marked Chestnuts	Discharge Weight
Radial-Dowel Wheel Separator							
	3223	7lb 6oz	100	3lb 4oz	3lb 2oz (CR) 3lb 2oz (DC)	94	7oz
	3223	9lb 2oz	94	3lb	3lb 12oz (CR) 2lb 9oz (DC)	85	10oz
	3223	-	-	-	-	-	-

Clogging was apparent in both the conveying region (CR) and deposit chamber (DC) despite the efforts of a self cleaning system. Frequently, chestnuts became lodged between the dowel rods on the spindle, causing a physical jam. The torque required to dislodge a stuck chestnut is undesirable when considering harvesting quality. Chestnuts also became stuck in the self cleaning apparatus itself. Because chestnuts differ in size and shape, spacing of fixed components becomes difficult. Slots designed for large chestnuts increase the opportunity for debris to fall through. Conversely, slots designed to limit the debris based on a smaller size, promote clogging. No suitable slot size or dowel rod spacing was determined to prevent clogging. Due to the addition of moving components and the clogging, the hypothesis was reformulated. Only two test runs were needed to reject this hypothesis.

Tests were run using the same RPM, compared to varying RPM's in the previous three chambers. The previous test results do not vary significantly for differing RPM's. The inlet air velocity was 7500 ft/min. A large inlet velocity was used to keep burs from becoming stuck in the conveying region. Although 7500 ft/min is larger than what was predicted, 4660ft/min, this design was deemed unsuccessful based on the high chestnut loss.

6.6 Deflection Separator

The design of the Deflection Separator, shown in Figure 20, consisted of 3/8 inch dowel rods mounted in the center of the conveying region, at an angle of 67.5 degrees with respect to the top of the chamber. Mounted on the sides of the conveying region are six deflectors. The deflectors have holes to allow air to pass. The first dowel is located 4 inches into the conveying region. Spacing for mounting the deflectors and dowel rods was selected to be 4 inches. This spacing was based on a full bur, partially opened, being less than four inches.

Chestnuts and debris entering the conveying region are subjected to momentum changes from impacting the obstruction devices. Chestnuts deflected from the air stream wind up in the deposit chamber. The bottom planes of the conveying region are angled to allow chestnuts to funnel back to the deposit chamber.

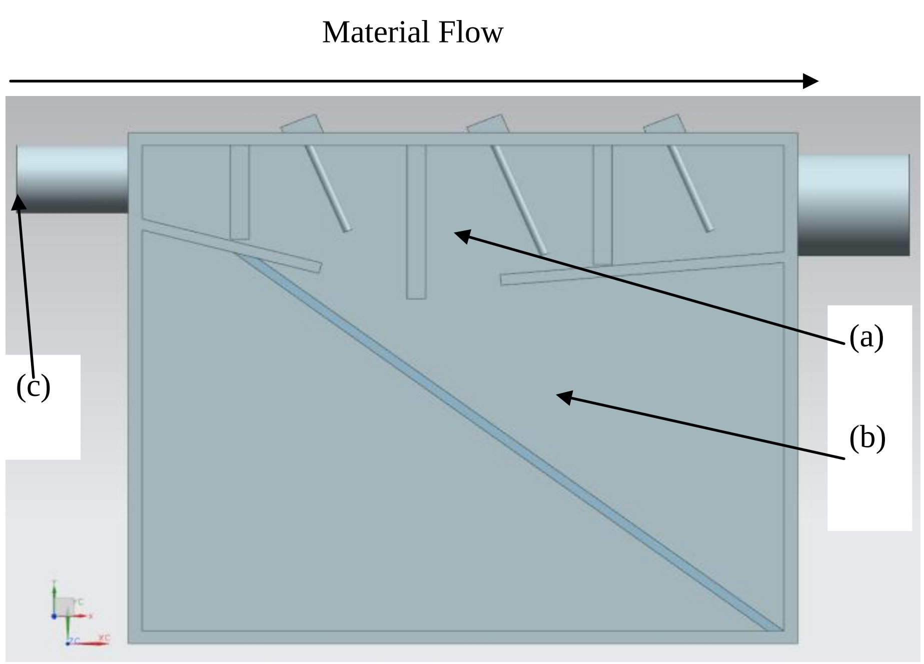

Figure 20. Deflection Separator: (a) conveying region, (b) deposit chamber and (c) inlet.

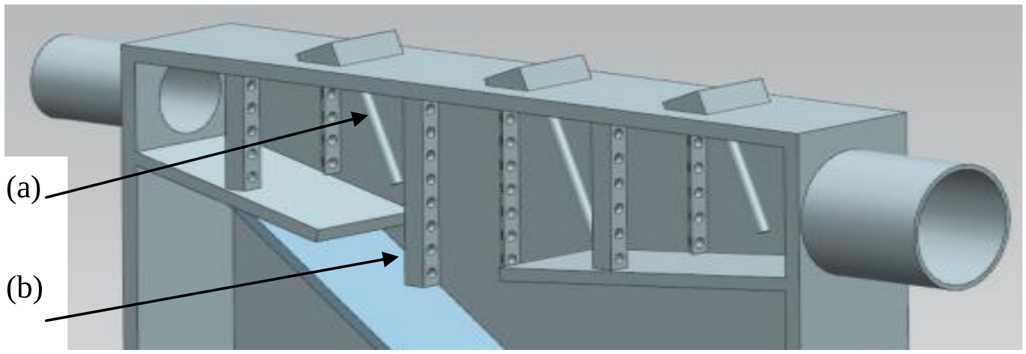

Figure 21. Deflection Separator conveying region with (a) dowel rods and (b) deflectors.

Table 9. Deflection Separator testing data.

		Material In			Collected		
	Engine RPM	Total Weight	Marked Chestnuts	Chestnut Weight	Weight	Marked Chestnuts	Discharge Weight
Deflection Separator	3003	7lb 9oz	100	3lb 14oz	3lb 7oz	94	3lb 8oz
					30% clogging		
	3003	8lb 8oz	94	3lb	4lb 10oz	94	3lb 5oz
					50% clogging		
	3003	7lb 12oz	94	3lb	3lb 8oz	86	3lb 14oz

Tests were run using the same RPM, compared to varying RPM's as with previous designs. The previous test results do not vary significantly for differing RPM's. A large inlet velocity was used to keep burs from becoming stuck in the conveying region. Frequently, debris became stuck in the conveying region. Spacing was allowed for individual burs however, during harvesting conditions burs are typically stuck together. These clusters caused clogging and the hypothesis was rejected.

6.7 Momentum Transfer Separator

The design of the Momentum Transfer Separator utilizes a sieve-type separation technique, as shown in Figure 22. This design considers the effects of conveying material at an angle. While dilute phase transport is desired, material separation and bed formation is still prevalent. Chestnuts and heavier materials were typically conveyed in the bottom half of a tube. Momentum transfer skids, mounted in the bottom of the conveying region, allow heavier material to drop from the air stream. Changing the momentum occurs when the chestnuts, or debris, strike the momentum skids. The skids are angled at 45 degree in reference to the direct line between the inlet and outlet of the chamber. A deflection point is added to the top surface, ensuring all material is obstructed. A separation grid, made of dowel rods, was mounted at the same 45 degree angle to separate chestnuts in the air stream beyond the deflection point. A declined plane is used to funnel material passing through the separation grid back to the deposit chamber.

Two sizes of burs were used during the testing of Momentum Transfer Separator: large debris (LD) and small debris (SD). Large debris is considered to be burs 4 inches or larger; small debris is anything less. The LD burs were collected from a chestnut orchard in early March 2011. Many of these burs fell post harvest and are not typical of harvesting season burs. The angled separation barriers and sorting grid did allow most burs to pass through the conveying region.

The chestnut recovery for the Momentum Transfer Separator was exceptional. In one test, one hundred percent of the chestnuts were captured in the sorting chamber: 97/97. Another test resulted in 96 out of 97 chestnut captured, as shown in Table 10. The chestnut loss in the Momentum Transfer Separator was significantly less than other designs, excluding the Air Flow

Separator, and was selected as the best design based on the performance criteria. The Air Flow Separator had no chestnut loss and 100% separation of material from the air stream.

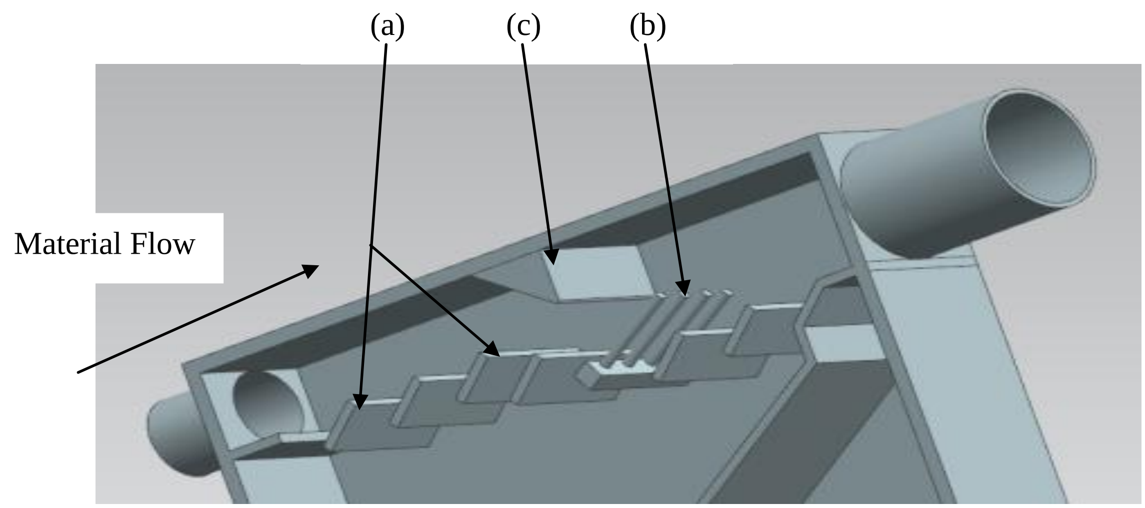

Figure 22. Momentum Transfer Separator: (a) momentum skids, (b) separation grid, (c) deflection point.

Table 10. Momentum Transfer Separator testing data.

		Material In			Collected		
	Engine RPM	Total Weight	Marked Chestnuts	Chestnut Weight	Weight (lbs)	Marked Chestnuts	Discharge Weight
Momentum Transfer Separator	3051	8lb 10oz (LD)	94	3lb 1oz	3lb 8oz	92	4lb 9oz
	3051	6lb 7oz (SD)	97	3lb 4oz	3lb 10oz	97	2lb 10oz
	3051	8lb 11oz (SD)	97	3lb 4oz	3lbs 11oz	96	4lb 6oz

Based on the results of the testing, the Momentum Transfer Separator met the initial criteria of minimizing chestnut loss with no clogging and was selected for further testing. The Saltation Sieve Separator (SSS) is the second phase of the Momentum Transfer Separator, which is different by the following: 1) a hinged paddle replaced the static deflection point and 2) the separation grid was replaced with a momentum transfer skid.

6.8 Saltation Sieve Separator (SSS)

The SSS is designed to remove chestnuts from an air stream by manipulating the momentum and the air velocity, and capitalizing on the effects. The SSS system is also designed to manipulate airflow, specifically forcing material interaction. Manipulating the air stream can produce a desired effect on what material can be conveyed; the saltation velocity differs for chestnuts and debris. The velocity of the air stream can be changed by installing orifices in the conveyance ductwork, either increasing or decreasing the air velocity. Likewise, obstructions or geometry changes can influence the flow behavior index, and also shift the maximum velocity point. In the case of the SSS system, shifting the maximum velocity point can be very advantageous when used in conjunction with conveyance.

Because chestnut separation is the overall goal, the SSS was designed to separate using obstruction devices to compliment dense phase bed formation, common in horizontal conveyance. Momentum transfer skids, shown in Figure 23, slope upwards and interact with chestnuts in the bed formation. The chestnuts in the bed are subjected to a physical interaction which decreases their momentum. Slots allow these chestnuts to fall from the air stream. While the bed is effectively being removed from the conveying tube, the geometry internal to the SSS changes slightly (diameter is increased), decreasing the air velocity. This is done to promote a fixed bed phase stage in the SSS. The SSS was designed to be mounted at an angle, relative to the ground, to influence and encourage bed formation in the conveying region.

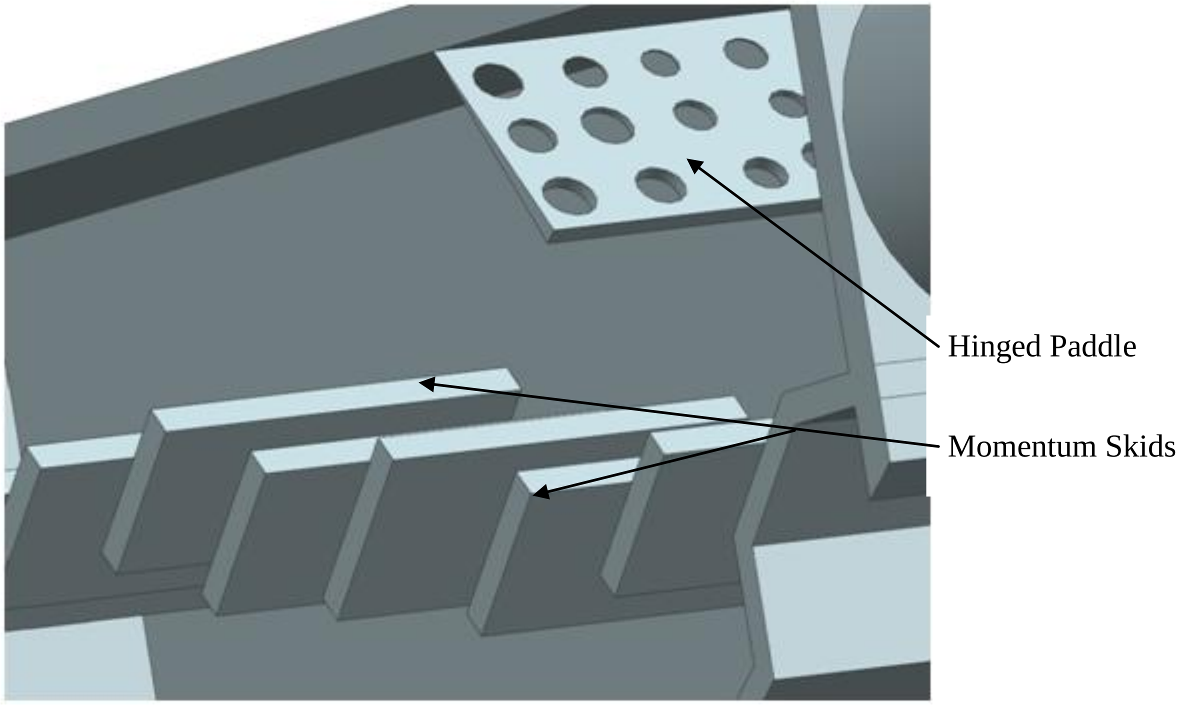

Figure 23. Saltation Sieve Separator conveying region.

Material in the top half of the conveying tube will experience particle to particle interaction and particle to wall interaction. Removing the bed gives the chestnuts in the upper air stream the chance to interact with the obstruction devices. A hinged sheet-metal paddle, shown in Figure 23, is mounted to the top of the conveying duct. This paddle ensures no material passes through the SSS without some forced interaction.

Conveyed material entering the SSS system encounters a change in boundary geometry which influences the air velocity, subsequently altering the aerodynamic relationships between the two. For sustained horizontal conveyance, the chestnuts must overcome the effects of the interactions with debris and the walls of the system. Two chestnuts colliding will experience a change in momentum, effectively slowing their conveyed velocity at that point in time.

Figure 24 Saltation Sieve Separator (SSS).

Figure 25 shows the momentum-transfer skids (a) and hinged paddle (b) location internal to the SSS system. The paddles was mounted in the conveying region, 6 in. upstream from the discharged port. Fourteen 1/2 in. holes were drilled into the obstruction paddle to allow airflow through the face. The paddle is mounted to the chamber with a standard 1 in. cabinet hinge and hardware. Weight was added to the paddle using a 3/8 in. bolt and four nuts to ensure the paddle disrupts the material and velocity profile during harvesting air flow conditions. Without the weight the paddle “opens”, or lays parallel to the air flow. A sliding door on the bottom of the chamber was used to extract sorted material from the harvested material, manually.

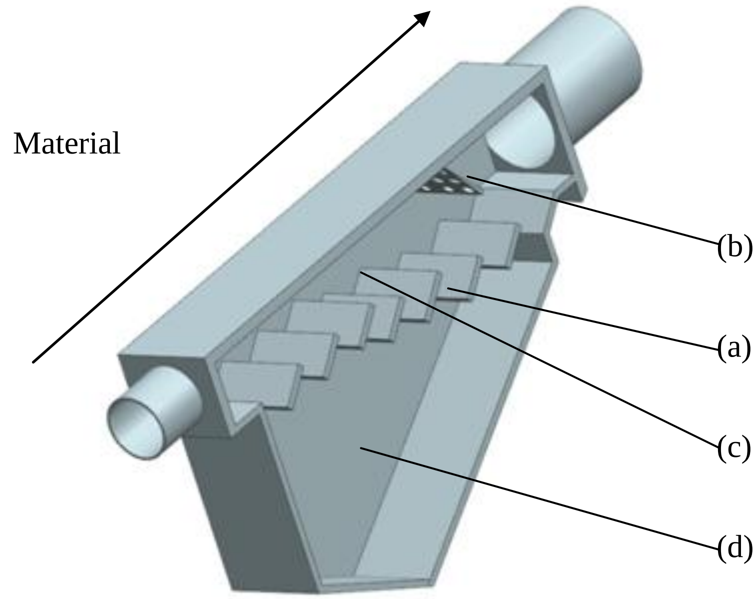

Figure 25. Saltation Sieve Separator components: (a) momentum skids, (b) hinged paddle, (c) conveying region, and (d) deposit chamber.

The momentum transfer skids are mounted internally to the sorting chamber, and constructed from 5/8” particle board. The dimensions are constant in two directions: 6 in. length and 5/8 in. thick. Widths range from 2.5 in. to 4 in. Because the momentum changes when material impacts the portion of the skid in the air stream, widths were chosen arbitrarily.

The Saltation Sieve Separator initially met our criteria for success. This design was chosen for further testing and evaluations.

7 Experiment Design

The harvesting performance of the final design (SSS) was evaluated based on the affects of three primary inputs: 1) the number of chestnuts entering the separation chamber, 2) the weight of debris and 3) the feed rate of material into the nozzle. The validation of the process was characterized by chestnut loss and separation efficiency.

The objective of the experiment was to determine the harvesting performance of the SSS as affected by the proportion of chestnuts and debris, and feed rate. Controlled quantities of chestnuts, marked with white paint, were added to each debris mixture. These marked chestnuts were of the variety Colossal and harvested in Michigan during the fall 2010 harvest. They were stored in cold refrigeration until testing. The debris was collected from a Michigan chestnut orchard in the spring of 2011. This debris was from the fall 2010 crop and had wintered on the orchard floor. The debris weight was measured before each test and compared to the weight of debris collected from the blower discharge. Any material blown from the collection bin was not considered a part of the total discharge weight. The nozzle feed rates were slow, medium, and fast. These depend upon the operator but a material density at the nozzle of low, medium, and high, were thought of as corresponding feed rate descriptions.

Table 11. Independent Variables and their levels

Independent Variables	Coded	Symbol Uncoded	Coded	Levels Uncoded
Number of Chestnuts	x1	Quantity	-1	20
			0	60
			1	100
Amount of Debris	x2	Weight	-1	1 lb.
			0	4 lbs.
			1	7 lbs.
Feed Rate	x3	Speed	-1	slow
			0	medium
			1	fast

A Box-Behnkin response surface design was used to set up and evaluate the experiment (Myers et. al. 2009). Three independent variables; number of chestnuts, weight of debris, and feed rate, were defined. The number of chestnuts was divided into three amounts: 20, 60, and 100. Chestnuts were not included or excluded, based on size or shape. Three levels of debris weight were used: 1 lb., 4 lbs., and 7 lbs. Nozzle feed rates were slow, medium, and fast, which are subjective depending upon the operator. Based on the principles of a Box-Behnken design for three independent variables, fifteen tests were suitable for analyzing the experiment. A run consisted of 15 tests and testing order was generated using R statistical analysis software. A total of 3 runs (45 tests) were made and each run order was sequenced randomly to further increase the accuracy of the experiment. The independent variables and their coded levels are shown in Table 11.

7.1.1 Performance Evaluations

The performance of the chestnut harvester was characterized by the following parameters.

7.1.1.1 Separation Efficiency

Separation efficiency was defined as the ratio of the weight of debris removed to the weight of debris which entered the SSS system, expressed as a percentage. Separation efficiency was computed as follows:

$$SepPer = \frac{DWin - DWdis}{DWin} \; x \; 100 \tag{9}$$

Where:

SepPer = Separation efficiency (%)

DWin = Weight of debris input (lbs.)

DWdis = Weight of debris discharged (lbs.)

7.1.1.2 Chestnut Loss

Chestnut loss was defined as the ratio of the number of chestnuts lost through the blower discharge to the number of chestnuts which entered the SSS system, expressed as a percentage. The following equation was used to calculate the chestnut loss:

$$C.L. = \frac{Ch\#in - Ch\#S.C.}{Ch\#in}\ x\ 100 \qquad (10)$$

Where:

C.L. = Chestnut loss (%)

Ch#in = Number of chestnuts input (qty.)

Ch#S.C. = Number of chestnuts collected in the separation chamber (qty.)

8 Results and Discussions

A second order polynomial was used for fitting the response surface to the experimental data. Contour plots of response surfaces for chestnut loss and separation percentage are shown in Figure 26 through Figure 31. The effects of the independent variables and their interactions on the performance criteria are shown in the analysis of variance tables; Table 13 and Table 14 are variance tables for chestnut loss and separation percentage, respectively.

Table 12. Testing data for chestnut loss and separation efficiency as a percentage

Variables			Separation Chamber		Discharge		
Number of Chestnuts	Debris Weight (lb)	Feed Rate	Total Weight (lb)	Number of Chestnuts	Debris Weight (lb)	Chestnuts Loss (%)	Separation Efficiency (%)
20	1	Medium	0.50	18.67	0.60	6.67	60.42
20	4	Fast	0.65	17.00	2.63	15.00	65.63
20	7	Medium	1.40	17.67	4.31	11.67	61.61
20	4	Slow	0.83	18.33	2.00	8.33	50.00
60	1	Slow	2.19	58.67	0.56	2.22	56.25
60	7	Slow	2.40	55.33	4.67	7.78	66.67
60	1	Fast	2.15	57.00	0.75	5.00	75.00
60	7	Fast	2.77	58.33	4.27	2.78	61.01
60	4	Medium	2.15	56.33	2.46	6.11	61.46
60	4	Medium	2.10	58.33	2.81	2.78	70.31
60	4	Medium	2.17	54.00	3.08	10.00	77.08
100	1	Medium	3.40	94.33	0.65	5.67	64.58
100	4	Slow	3.90	96.00	3.25	4.00	81.25
100	7	Medium	3.71	94.00	4.73	6.00	67.56
100	4	Fast	4.02	98.67	2.56	1.33	64.06

8.1 Chestnut Loss

Machine chestnut loss data are presented in Table 12. The analysis of the regression is given in Table 13. According to the regression analysis, the estimated coefficients for the feed rate and the weight of debris have low confidence levels. The only significant variable affecting chestnut loss was the number of chestnuts, with a 97 percentage confidence for the estimated coefficient. The feed rate and the number of chestnuts interaction coefficient was estimated at an 80% confidence level.

Table 13. Analysis of variance table for chestnut loss data

Coefficients	Estimate	Std. Error	t value	Pr(>|t|)
(Intercept)	6.3000	1.7819	3.5350	0.0166
x1: Number of Chestnuts	-3.0813	1.0912	-2.8240	0.0369
x2: Debris Weight	1.0837	1.0912	-1.0912	0.3662
x3: Feed Rate	0.2200	1.0912	0.2020	0.8482
x1 : x2	-1.1675	1.5432	-0.7570	0.4834
x1 : x3	-2.3300	1.5432	-1.5100	0.1915
x2 : x3	-1.9450	1.5432	-1.2600	0.2632
x1^2	1.9588	1.6062	1.2190	0.2770
x2^2	-0.7662	1.6062	-0.4770	0.6534
x3^2	-1.0888	1.6062	-0.6780	0.5280

Multiple R-squared: 0.7596　　Adjusted R-squared: 0.3268

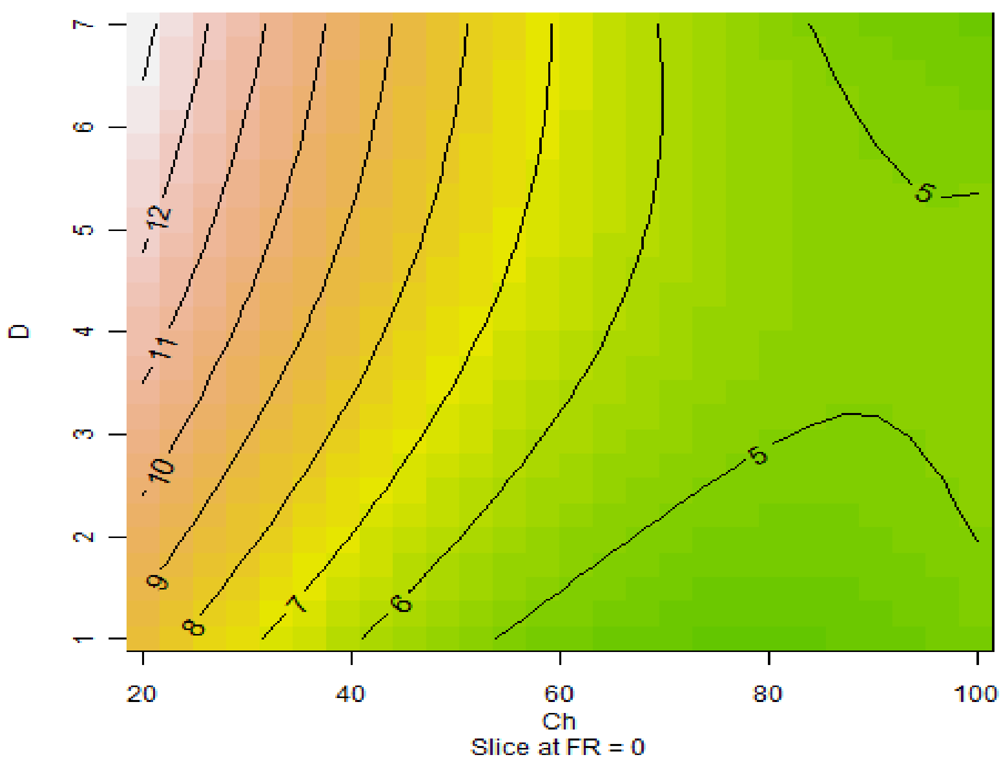

Figure 26. Chestnut loss percentage as affected by the number of chestnuts (Ch) and weight of debris (D).

Figure 26 is a contour plot for the response surface for chestnut loss based on the interaction between the number of chestnuts (Ch) and the weight of debris (D). It is sliced or viewed from the feed rate (FR) set equal to medium speed. Between 80 and 100 chestnuts, the influence of the weight of the debris has little effect on the chestnut loss percentage. However, when the weight of the debris increased the chestnut loss increased from 8% to 13%, when 20 chestnuts were input. The maximum chestnut loss occurred at low chestnut numbers. The chestnut loss for the SSS system can be minimized by increasing the density of the chestnuts going through the system.

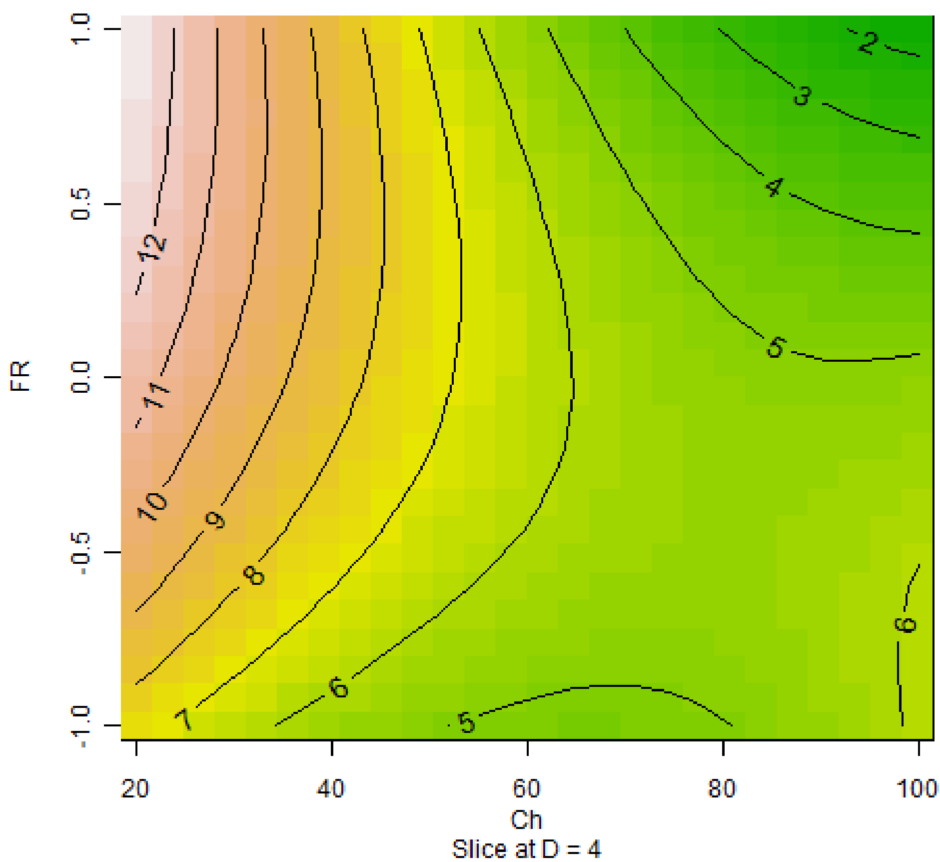

Figure 27. Chestnut loss as affected by the number of chestnuts (Ch) and the feed rate (FR).

Figure 27 is a contour plot for the response surface for chestnut loss based on the interaction between the number of chestnuts (Ch) and the feed rate (FR). It is sliced or viewed from the weight of debris (D) set equal to 4 lbs. The maximum chestnut loss occurs at low chestnut numbers with a fast feed rate. Chestnut loss is minimized when the number of chestnuts is above 60 which ranged from 2-6%. This suggests that when a larger number of chestnuts enter the SSS system, regardless of feed rate, the chestnut losses will be minimized.

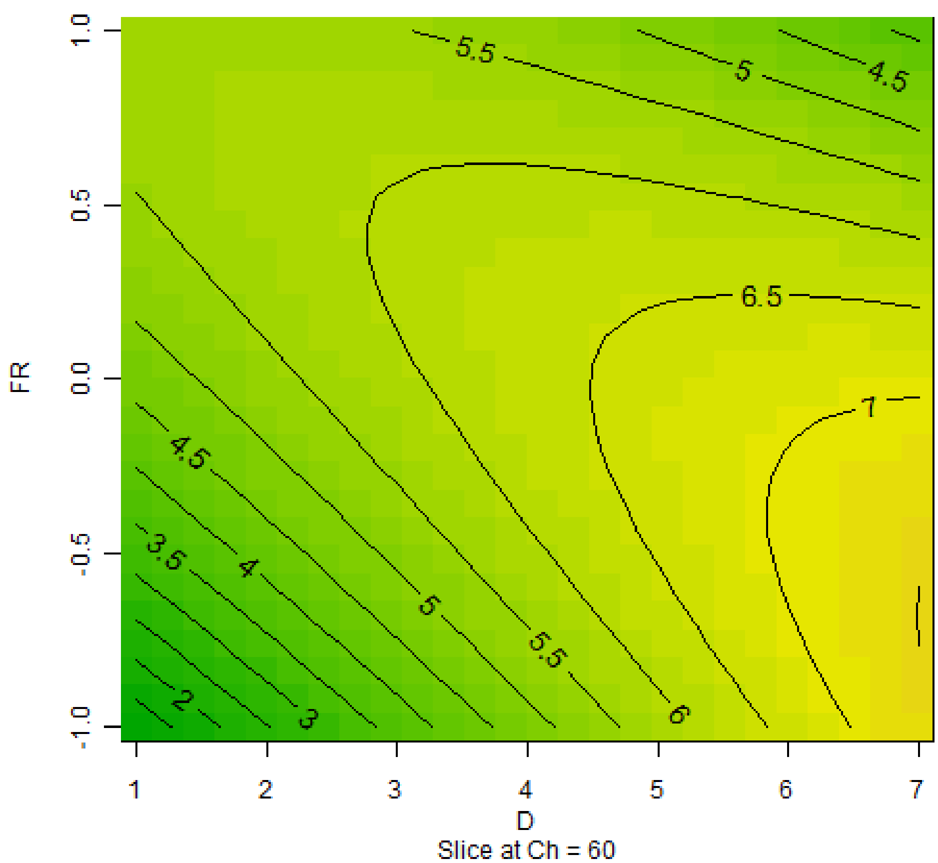

Figure 28. Chestnut loss as affected by weight of debris (D) and feed rate (FR).

Figure 28 is a contour plot for the response surface for chestnut loss based on the interaction between the weight of debris (D) and the feed rate (FR). It is sliced or viewed from the number of chestnuts (Ch) set equal to 60. The chestnut loss varies from 2.5% at a low debris weight and a low feed rate, to 8% at a high debris weight and low feed rate.

8.2 Separation Efficiency

The analysis of the regression is given in Table 14. According to the regression analysis, the estimated coefficients for the number of chestnuts and the weight of debris have low confidence levels. The most significant variable affecting the separation efficiency was for the feed rate, with a 98% confident estimated coefficient. The number of chestnuts and the feed rate interaction coefficient was estimated with a 96% confidence level. Contour plots of the response surfaces for separation efficiency are shown in Figure 29-15. The separation efficiency for the SSS system ranged from 50% to 81%.

Table 14. Analysis of variance table for separation efficiency data

Coefficients	Estimate	Std. Error	t value	Pr(>|t|)
(Intercept)	50.873843	10.792602	4.714	0.00527
x1 : Number of Chestnuts	0.307292	0.275318	1.116	0.31511
x2 : Debris Weight	2.662037	3.422283	0.778	0.47184
x3: Feed Rate	22.208333	6.756855	3.287	0.02179
x1 : x2	0.002083	0.026462	0.079	0.9403
x1 : x3	-0.20625	0.079386	-2.598	0.04836
x2 : x3	-2.083333	1.058475	-1.968	0.10616
x1^2	-0.001589	0.002066	-0.769	0.47662
x2^2	-0.337963	0.367232	-0.92	0.39964
x3^2	-1.541667	3.305089	-0.466	0.66051
Multiple R-squared: 0.778			Adjusted R-sqaured: 0.3779	

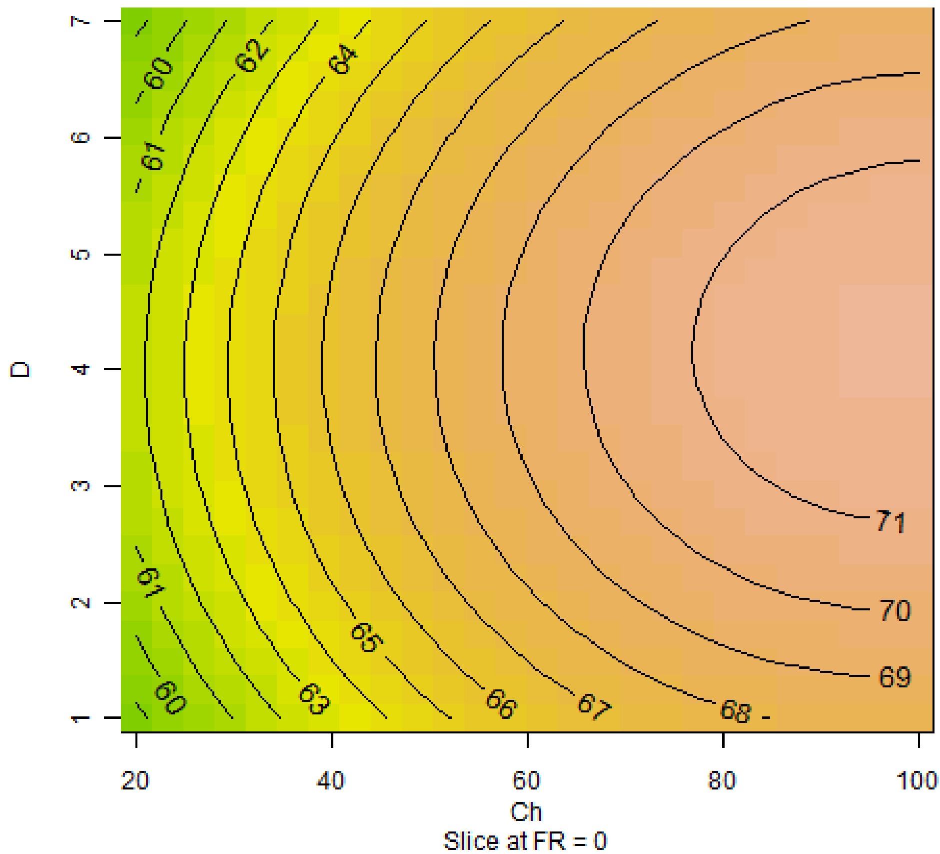

Figure 29. Response surfaces for separation efficiency as affected by number of chestnuts (Ch) and weight of debris (D).

Figure 29 is a contour plot for the response surface for separation efficiency based on the interaction between the number of chestnuts (Ch) and the weight of debris (D). It is sliced or viewed from the feed rate (FR) set equal to medium speed. The maximum separation efficiency occurs at 100 chestnuts and 4 lbs. of debris, and appears as a mound or peak in Figure 29. The separation efficiency decreases as the number of chestnuts decreases because of the characteristic of dense phase conveyance, specifically where debris is conveyed. During dense phase conveyance, the heavier material is conveyed along the bottom portion of the tube, essentially forcing the lighter material higher in the air stream, or top of the tube. When the number of chestnuts is low, the debris has more opportunity to travel throughout the entire diameter of the tube, and will interact with the momentum skids. More debris separation occurs when the number of chestnuts is low.

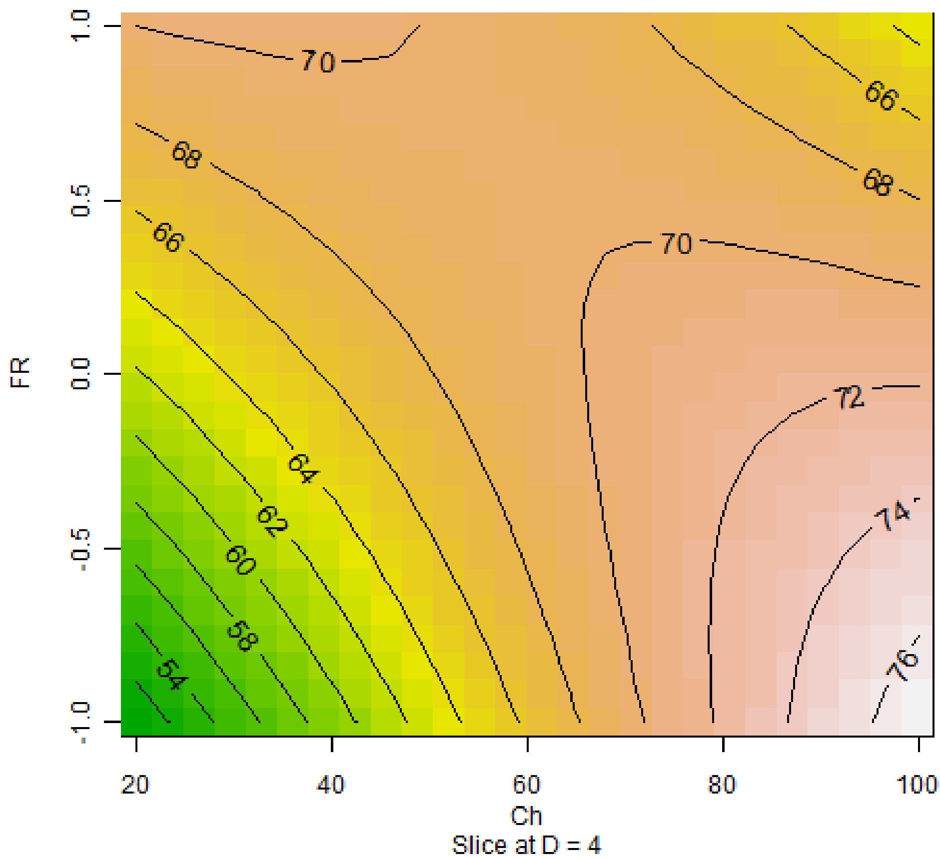

Figure 30. Separation efficiency as affected by the number of chestnuts (Ch) and feed rate (FR).

Figure 30 is a contour plot for the response surface for separation efficiency based on the interaction between the number of chestnuts (Ch) and the feed rate (FR). It is sliced or viewed from the weight of debris (D) set equal to 4 lbs. The maximum separation efficiency occurs at a 100 chestnuts and low feed rate; maximum separation efficiency over 75% was achieved. When

20 chestnuts were fed into the SSS slowly, the separation efficiency decreased. The separation efficiency generally decreased as the number of chestnuts decreased.

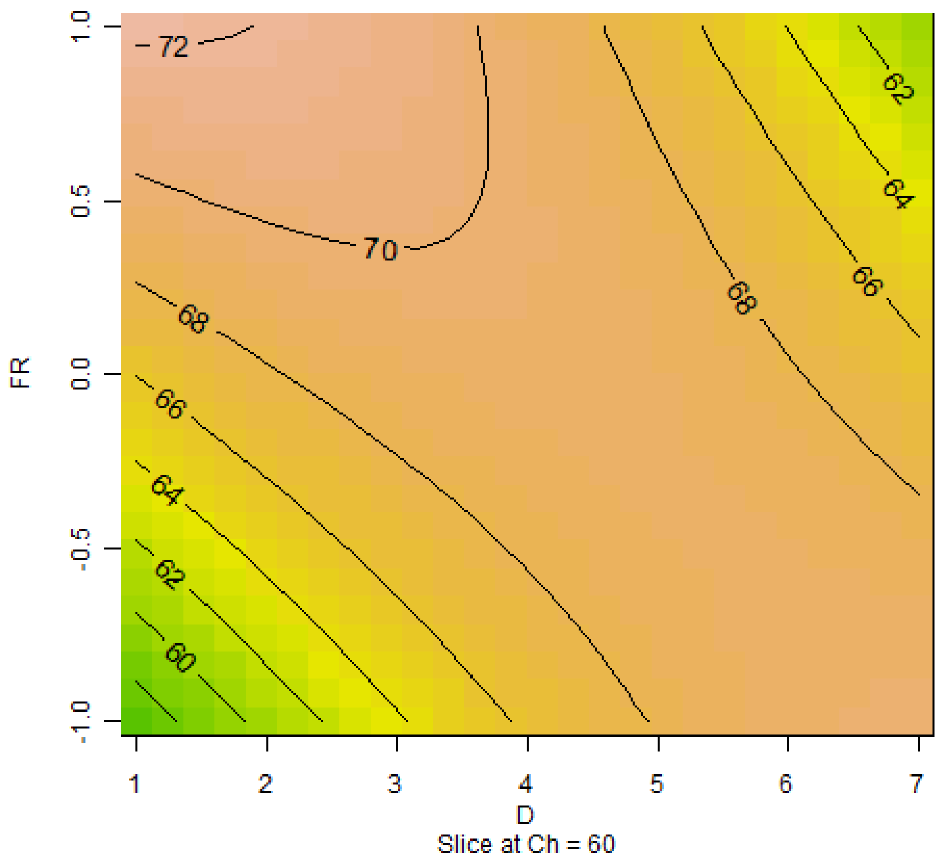

Figure 31. Separation efficiency as affected by weight of debris (D) and feed rate (FR).

Figure 31 is a contour plot for the response surface for separation efficiency based on the interaction between the weight of debris (D) and the feed rate (FR). It is sliced or viewed from the number of chestnuts (Ch) set equal to 60. A ridge of maximum separation efficiency occurs across the contour plot. When the weight of debris is 1 lb., maximum separation efficiency is at a large feed rate. When the weight of debris is 7 lbs., the maximum separation efficiency is at a low debris weight. The maximum SSS separation efficiency ridge includes a medium feed rate and 4 lbs. of debris, or middle range for each variable.

In addition to the multiple variable regression analysis, regression analysis was used to investigate the chestnut loss solely based on the interaction between the number of chestnuts and the feed rate. Table 15 shows the linear regression analysis for the chestnut loss based on the number of chestnuts and the feed rate. The model coefficient describing the interaction between the number of chestnuts and the feed rate was estimated at a 98% confidence level. The model coefficient for the number of chestnuts entering the SSS system was estimated at a 96% confidence level.

Table 15. Linear regression analysis for chestnut loss based on the number of chestnuts and feed rate.

Coefficients	Estimate	Std. Error	t value	Pr(>|t|)	
(Intercept)	65.5260	1.6020	40.9000	2.2700E-13	***
x1: Number of Chestnuts	4.9740	2.1940	2.2670	0.0445	*
x3: Feed Rate	1.4410	2.1940	0.6570	0.5247	
x1 : x3	-8.2050	3.1020	-2.6450	0.0228	*

Multiple R-squared: 0.5332 Adjusted R-squared: 0.4059
Signif. codes: 0 ‘***’ 0.001 ‘**’ 0.01 ‘*’ 0.05 ‘.’ 0.1 ‘ ’ 1

Ninety five percent of the time, the chestnut loss model can be used to describe the chestnut loss in the SSS system. The equation for chestnut loss is:

$$Chestnut\ Loss = 65.526 + 4.974 * X1 + 1.4410 * X3 - 8.2050 * X1 * X3 \qquad (11)$$

9 Conclusions

The SSS technique used for harvesting chestnuts can be successfully employed as a single-stage chestnut harvesting system. Chestnut losses average 4-5% when a large number of chestnuts were entering the SSS system. The separation efficiency was the highest when a large number of chestnuts were entering the SSS system at a slow feed rate. This characteristic is advantageous for growers, or processors, to maximize separation efficiency while minimizing chestnut losses.

Because the average size orchard in Michigan is 5 acres, a grower producing 1500 lbs/acre could economically purchase a machine which costs $6,000.00. The SSS system and its single-stage design presents a potentially economically feasible harvesting system for Michigan chestnut growers.

10 Future Research

Future research for the SSS system is needed for optimization. Realizing that this system is a foundation to be built upon, the author suggests some further ideas for research. A harvesting challenge still facing chestnut growers is what should be done with chestnuts that are contained inside burs. The growers and industry have not determined or set a standard to the quality of these chestnuts. The SSS system does not remove chestnuts inside of burs specifically. A pre-treatment process to shuck the chestnut from the burs may be a solution, assuming growers and the industry want to harvest these chestnuts.

1. Testing the performance parameters when the system is up-scaled to larger capacities: 10, 15, and 20 acres.

2. Adding dual hose suction ports to increase harvesting capacity.

3. Testing the performance parameters when the system is installed in conjunction with a windrowing or ground collection system versus no pre-processing based harvesting.
4. Evaluation of chestnut quality for chestnuts harvested using the SSS technique compared to hand harvesting and mechanical harvesting.
5. Testing the SSS system for other products or processes where a single-stage system can improve performance or efficiency.

APPENDICIES

11 Appendix A: Engine hp and Air Flow calculations

```
%% Pressure Drop Calculations for Chestnut Harvester    %


%-------------------------------------------------------%
% This program calculated the total pressure drop for   %
% a defined geometric systems, based on the aerodynamic %
% properties of chestnuts and standard air.  Horsepower %
% requirement is the desired output.                    %
%                                                       %
% Mark De Kleine                                        %
% January 2011                                          %
%                                                       %
%-------------------------------------------------------%
close all; clear all;

%% Defining Variables
% Design Requirements
Vc = 23.8; %                        - Conveying Velocity (m/s)
Vol = 2.45; %                       - Air volume (m/s)

% Standard Air Properties and Gravity
p_air = 1.2; %                      - Air Density (kg/m^3)
g = 9.81; %                         - Gravity (m/s^2)
u_air = 10^-5; %                    - Air Viscosity (kg m/s)

% Properties of Chestnuts
pc = 531; %                         - Bulk Density (kg/m^3)
d = 0.035; %                        - Chestnut Diameter (m)
Pp = 1135.68; %                     - Chestnut Density (kg/m^3)

% Chamber Design Configuration
D = 0.1016; %                       - Tube diameter (m)
delta_z = 1.5; %                    - Vertical height lift (m)
k = 0.9; %                          - Fitting Loss Coeff. Srivastava et al.
numb_bends = 3; %                   - Number of Bends in system
L = 7; %                            - Length of Conveying duct (m)
R_D = 1.05; %                       - Radius to Diameter Ratio
n_b = 0.6; %                        - Blower efficiency

%% Capacity
% Maximum Capacity from Economic Analysis
acres = 9.3; %                      - Number of Acres (ac)
lb = 3000; %                        - Pounds of Chestnuts per Acre (lbs)
days = 2; %                         - Days between harvest (days)
wk_hrs = 8; %                       - Hours in a standard work day (hrs)
kg_conv = 0.454; %                  - conversion to kilogram
hr_conv = 3600; %                   - conversion to seconds

% Bell Curve Percent
perc = .2; %                        - Bell Curve Percentage fallen between
days
```

```
Cap= (((((acres * lb)/ days) * perc) / wk_hrs) * kg_conv) / hr_conv; %kg/s


%% Mass Flow Rate
Q = (pi/4)* D^2 * Vc; %              - Volumetric Flow Rate (m^3/s)
CFM = Q * 35.3 * 60; %               - 35.3 ft^3/m^3 and 60s/1min (ft^3/s)

m_dot = p_air * Q; %                 - Mass Flow Rate (kg/s)

theta_m = Cap / m_dot; %             - Mass Flow Ratio

%% Reynolds Number Calculation
N_rc = (p_air * Vc * D) / u_air;

%% Line Pressure Loss
lamda = 4 *(0.0014 + 0.125*(N_rc^-0.32)); %          - Line Friction Factor

P_lin = lamda * (p_air / 2) * (Vc ^2) * (L / D);%    - Pressure Loss (Pa)

%% Acceleration Pressure Loss
% To get Velocity of solids:
Vs = Vc *(1 - 0.68*(d^0.92)*(Pp^0.5)*... %           - Solids Velocity (m/s)
    (p_air^-0.2)*(D^0.54));

P_acc = theta_m * Vc * p_air * Vs; %                 - Pressure Loss (Pa)

%% Lift Height Pressure Loss
p_star = theta_m * Vc * p_air / Vs;

P_vrt = p_star * g * delta_z; %                      - Pressure Loss (Pa)

%% Pressure Drop due to Solids and Particle Interaction
lamda_s= (0.0285 * sqrt(g*D)) / Vc;

P_spi = theta_m*lamda_s*(p_air/2)*(Vc^2)*(L/D);%     - Pressure Loss (Pa)

%% Pressure Loss due to Bends
% Equivalent Length
Leq = (k * D) / lamda;%                              - Equivalent length for
bends
Leq_b = numb_bends * Leq;

P_bnd = (P_lin * Leq_b) / L;%                        - Pressure Loss (Pa)

%% Pressure Loss due to Solids

P_sol = p_air * (Vc^2) *(0.245 *... %                - Pressure Loss (Pa)
    (m_dot / (p_air * Vc * D^2)) * (R_D^-.26));


%% Total Pressure Loss

P_tot = P_lin + P_acc + P_sol + P_bnd + P_spi + P_vrt;% - Pressure Loss (Pa)
```

```
%% Power Requirements
Pwr_hp = ((P_tot * Q) / n_b) *(1.34/1000); %        - Blower power needed
(hp)
```

12 Appendix B: Velocity Profiles

An Alnor Velometer, series 6000P, was used for measuring air velocity at several locations throughout the harvesting system. Measurements were taken at varying depths to quantify the velocity profile and examine the air stream size. The velocity profiles were plotted for each test. These figures are outlined below.

A Velleman DM6234 digital tachometer is used to measure the engine drive shaft rpm and blower drive shaft rpm. A piece of reflective tape is added to each shaft at the rpm measurements point.

12.1 B.1: Air Flow Separator

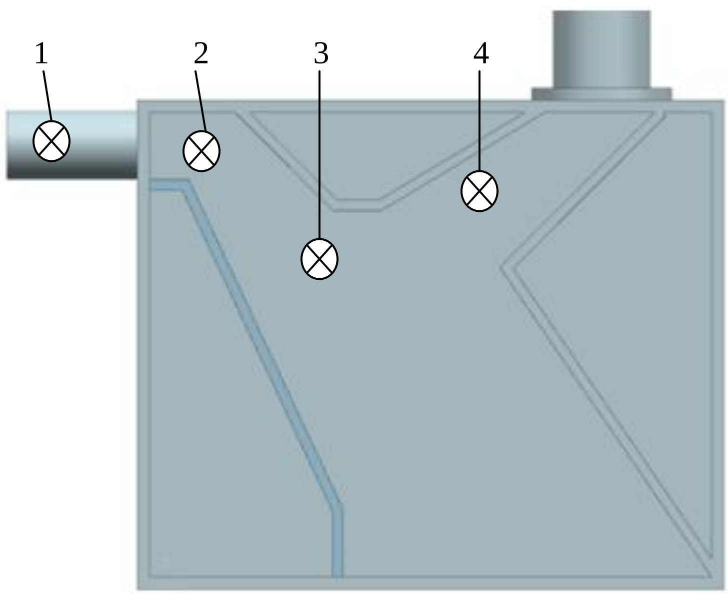

Figure B.32. Velocity measurement positions in the Air Flow Separator.

Table B.16. Air Flow Separator air velocities.

Engine shaft RPM	1580	2580	3010
Fan Shaft RPM	928	1500	1777
	Velocity Measurements (ft/min)		
Inlet tube	5000	6500	7400
Position 1 (in)			
1	3000	1800	3800
3	4000	4800	4800
4	1800	5000	7000
5	0	2600	3200
Position 2 (in)			
1	2200	5200	5400
3	1100	2600	5000
5	0	0	2000
7	0	0	0
9	0	0	0
Position 3(in)			
1	3000	5000	5800
2	1600	2400	6000
3	800	1500	3000
5	0	1000	1800
7	0	1000	1800
Position 4 (in)			
1	1100	1200	1800
2	1300	1400	2200
3	800	1200	2000
5	0	300	1000
Outlet (in)			
1	3000	4100	4600
2 at Focus	3000	4800	5000
2 at Wall	2100	3700	3200

The positions at which the air velocity was taken are shown in Figure B.32. The y-value of depth is measured from the top of the air flow chamber. The x-values were located at key points of interest and can be found in **Error! Reference source not found.**. The air velocity measurements were taken in the middle of the air stream, along the third dimension or z-axis. The following graphs represent the air layer geometry in the cross section of the chamber.

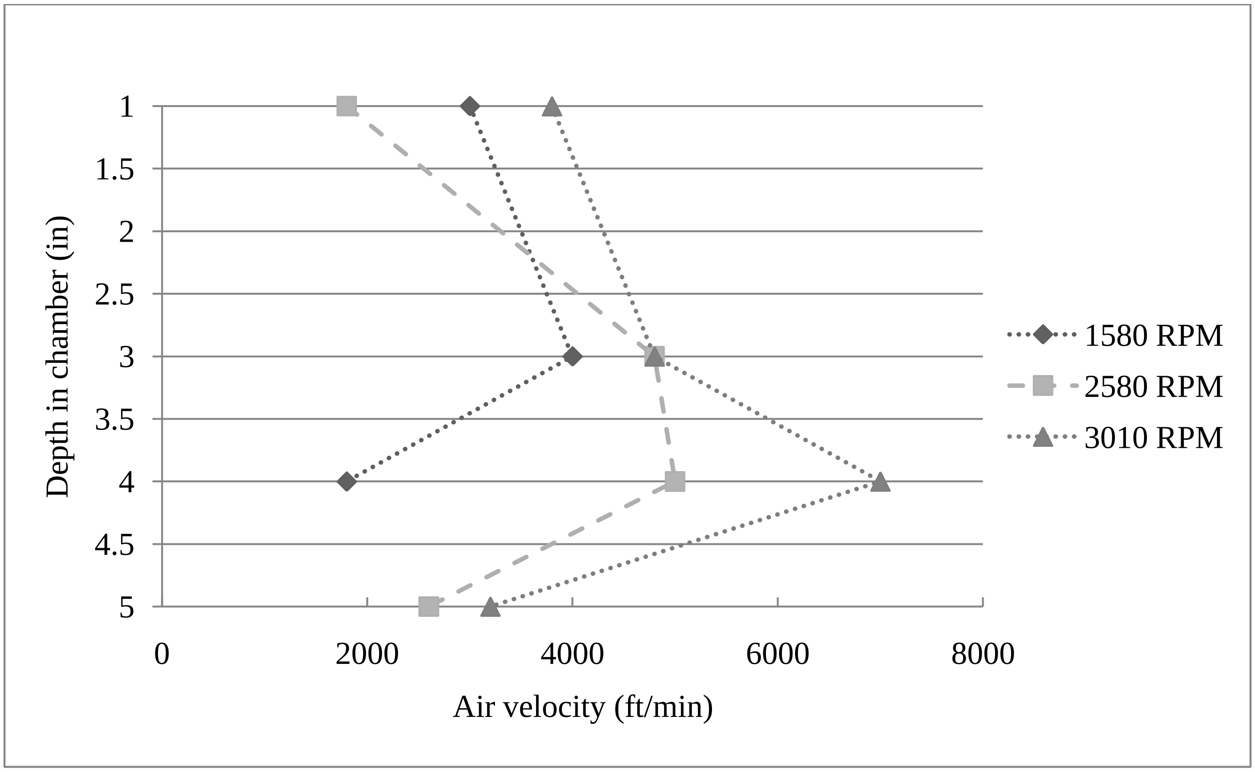

Figure B.33. Air Flow Separator air velocities at position 1.

At position 1, the maximum velocity point shifts downward, or further down from the top of the chamber, as the RPM and air velocity are increased. The maximum velocity point shifted downward 1 inch when the engine RPM doubled. Negative pressure air flow becomes more streamlined as the velocity increases; that is, non plug-like flow. As the air particles move faster away from each other, the air layer shrinks and the maximum velocity point becomes more distinguishable, as in the 3010 RPM velocity profile.

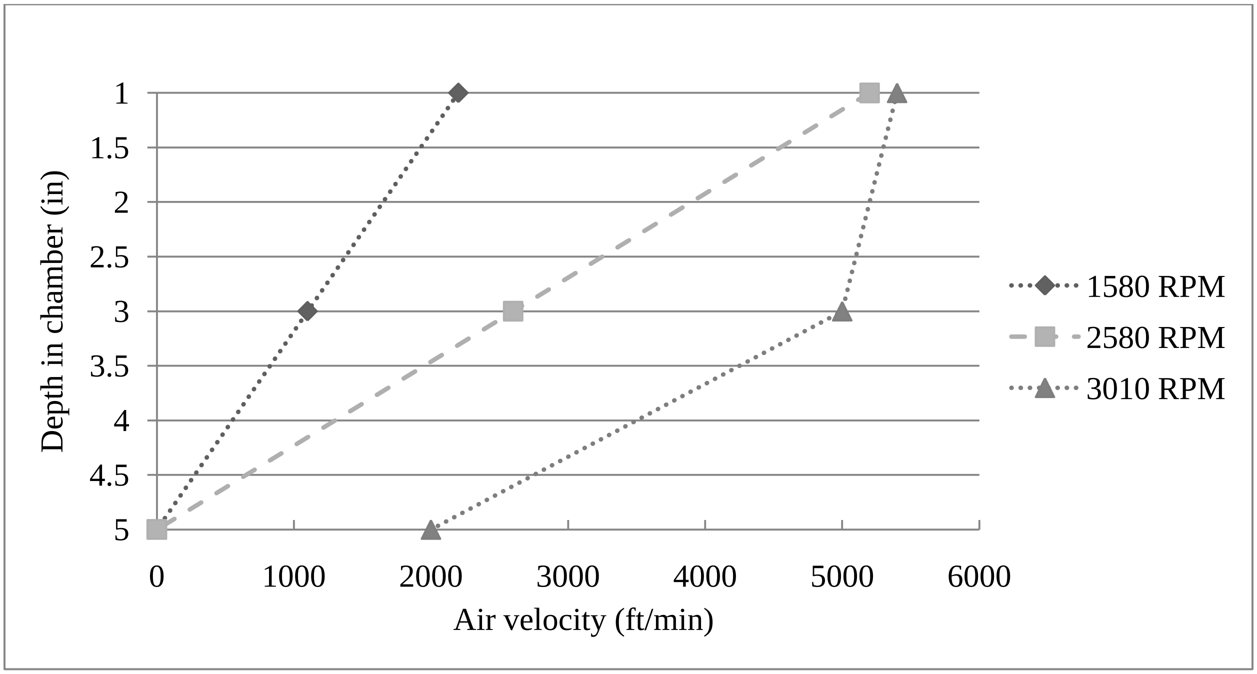

Figure B.34. Air Flow Separator air velocities at position 2.

At position 2, the maximum velocity point is at the top of the air chamber. This is unintuitive based on the air profile described at position 1. The complexity of an air flow problem is apparent here. As air is transitioning from position 1 to position 3, it passes through position 2 where the air stream is bending and curving through the chamber. The maximum velocity point can be shifted using geometry.

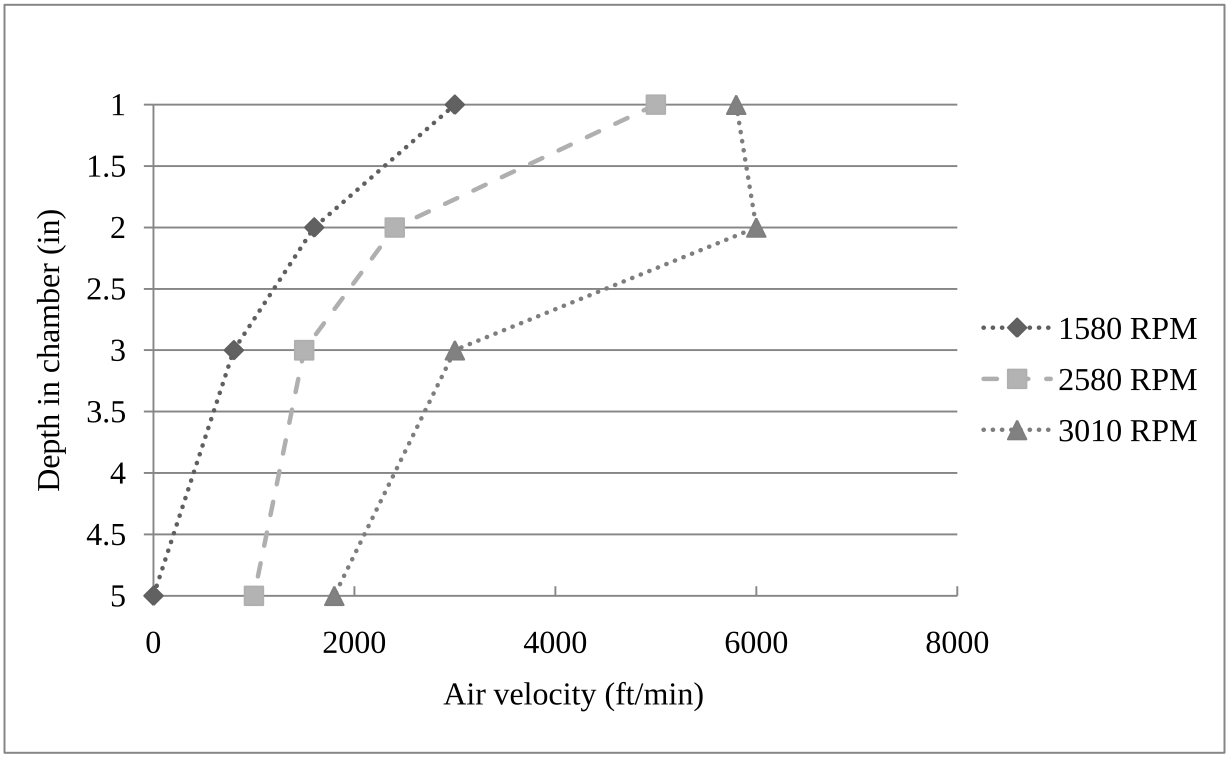

Figure B.35. Air Flow Separator air velocities at position 3.

The air velocity profiles for the Air Flow Separator at position 3 are depicted in Figure B.35. The top side of the conveying region has the largest velocity for all three RPM settings. The increase in air velocity is related to the geometry of the chamber and airflow characteristics around bends. Measurements taken at position 3 show the air layer shrinkage at the top of the air chamber.

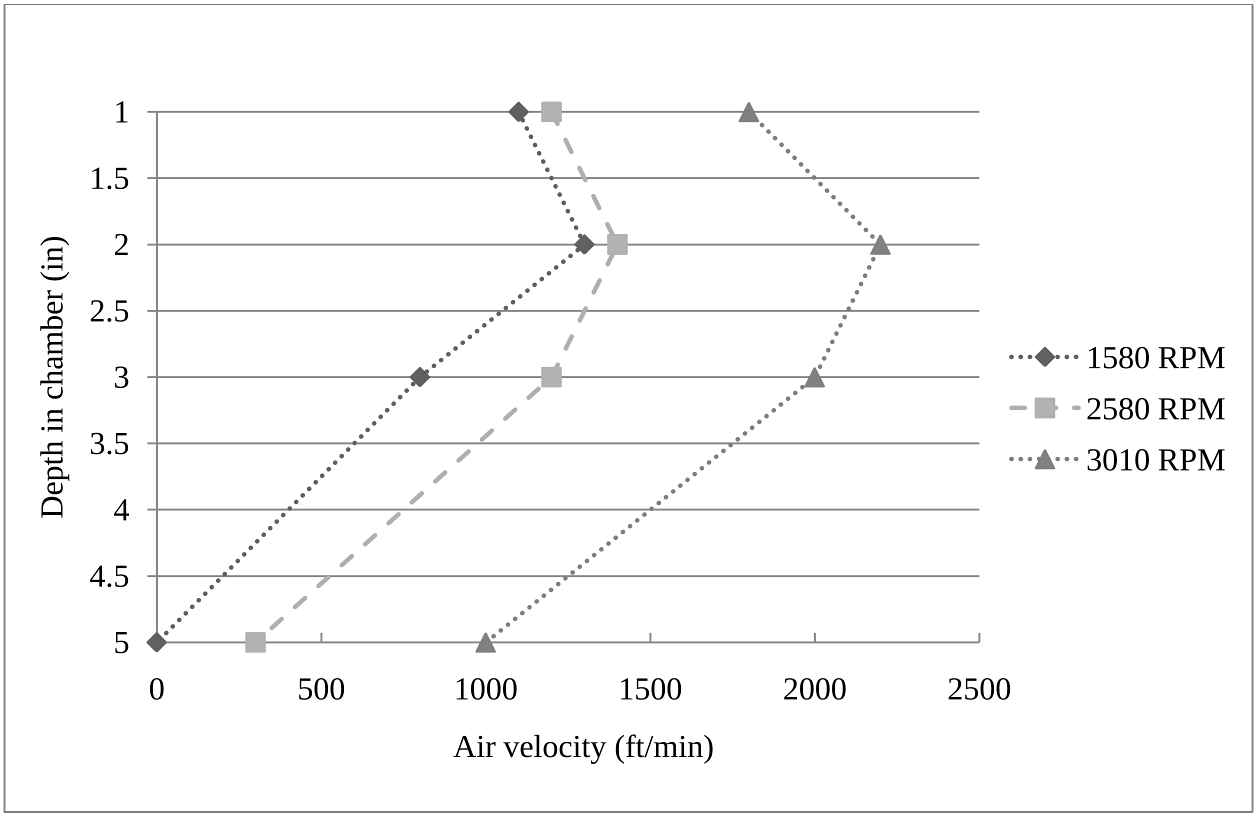

Figure B.36. Air Flow Separator air velocities at position 4.

At position 4, the velocity profiles resemble a standard pipe flow profile and are similar throughout. The highest velocities were more towards the top of the chamber.

12.2 B.2: Dowel Grid Separator

The velocity profiles for the Dowel Grid Separator at varying positions are depicted in the following figures. Figure B.37 show the positions at which the air velocities were measured.

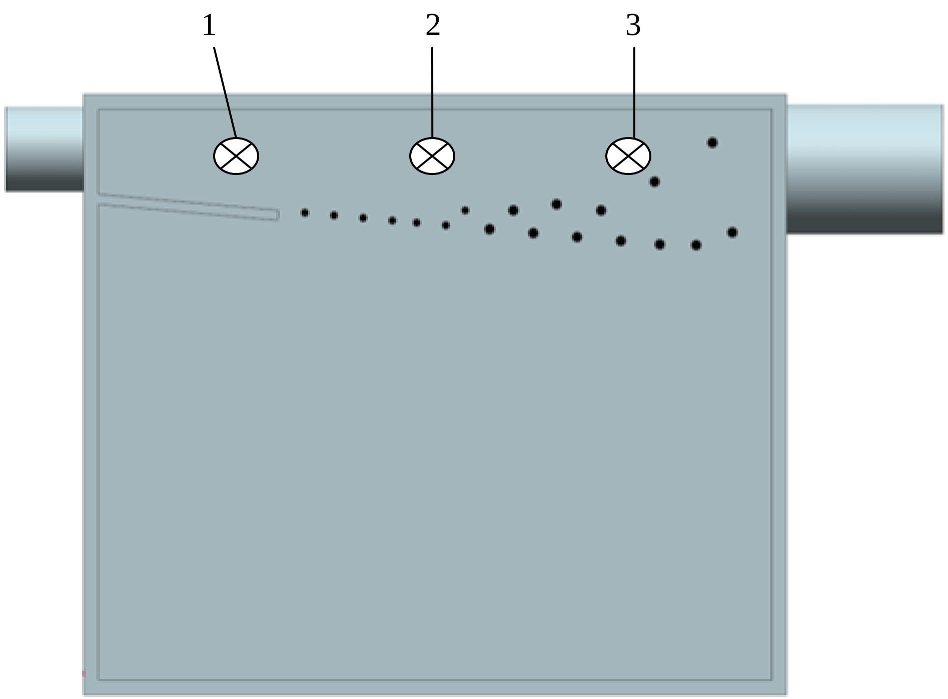

Figure B.37. Dowel Grid Separator air velocity measurement positions.

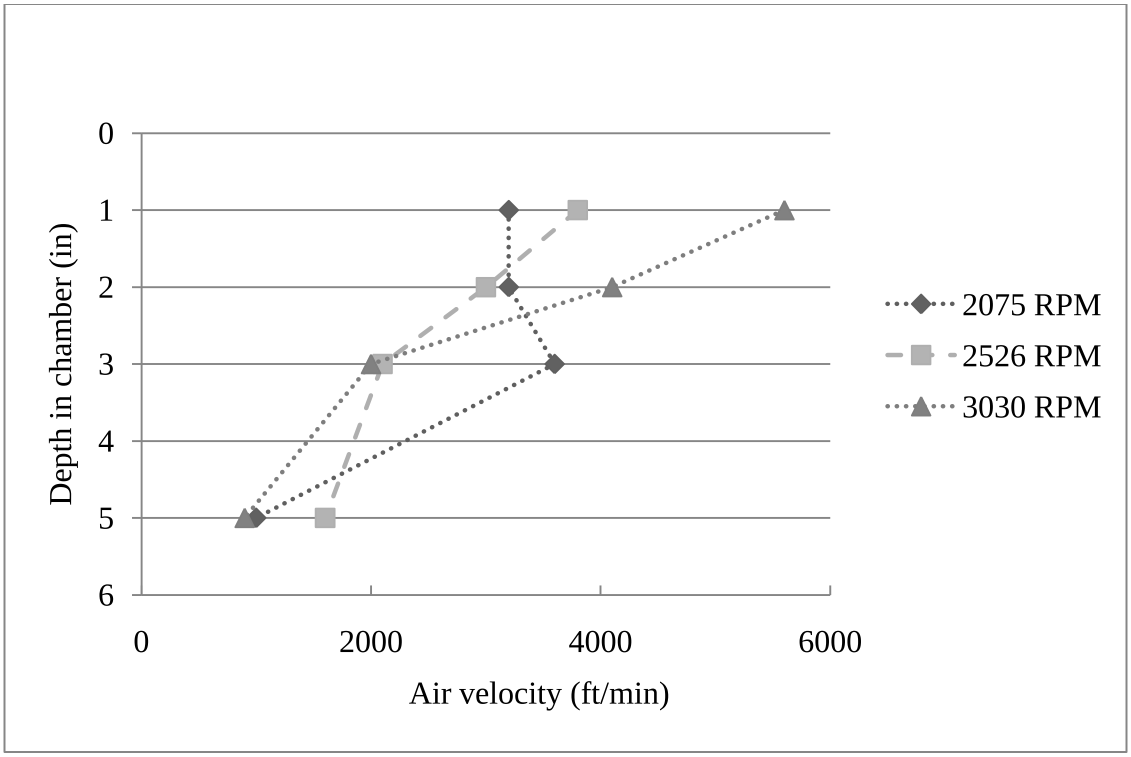

Figure B.38. Dowel Grid Separator air velocities at position 1.

The air velocity profile for the Dowel Grid Separator at Position1 remains relatively constant across the spectrum of tests. The lowest engine RPM had the highest velocity 3 inches below the top of the chamber. There is no explanation for this; human error while taking data was possible.

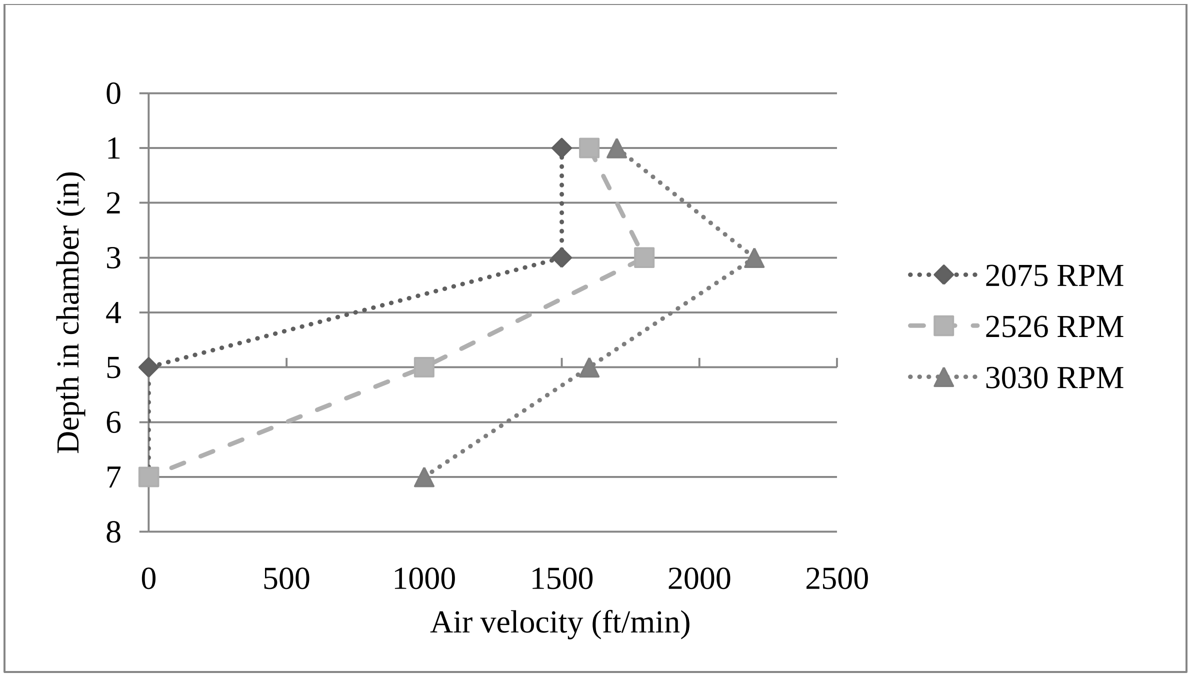

Figure B.39. Dowel Grid Separator air velocities at position 2.

The air layer profile for the Dowel Grid Separator at position 2 is shown in Figure B.39. As the engine RPM increased each air layer profile increased accordingly. There was no significant shift in the depth of the maximum velocity point between any air profiles at position 2.

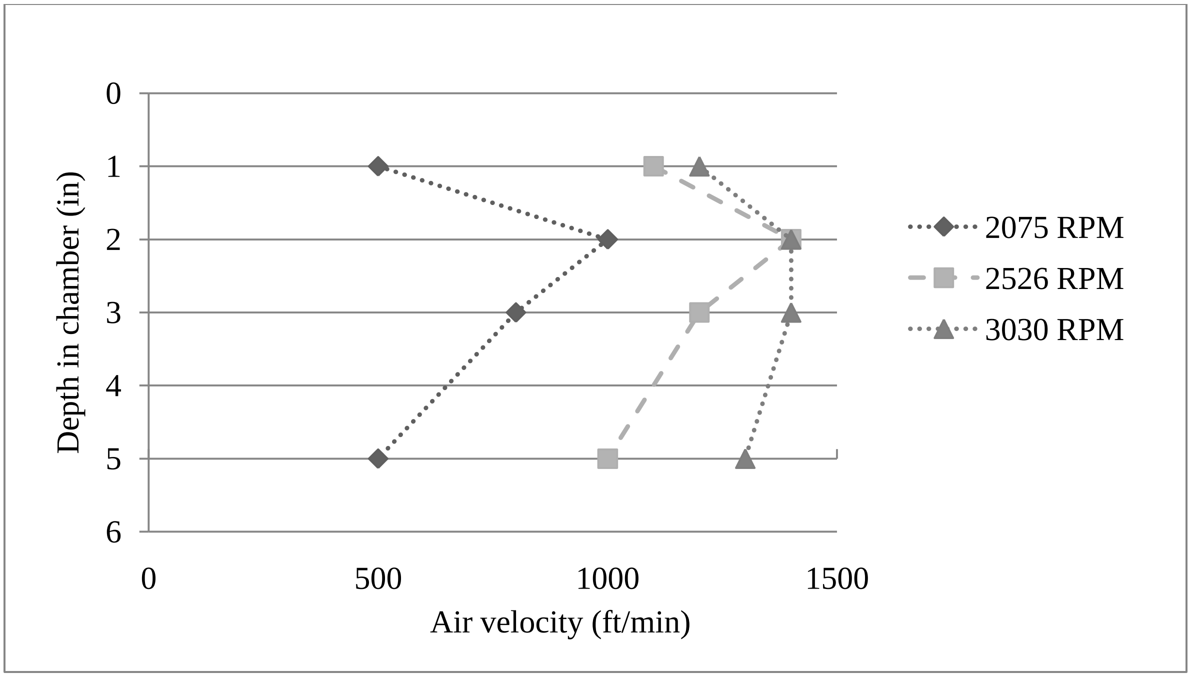

Figure B.40. Air Flow Separator air velocities at position 3.

Table B.17. Dowel Grid Separator air velocities.

Engine shaft RPM	2075	2526	3030
Fan Shaft RPM	1230	1479	1828
Velocity Measurements (ft/min)			
Focus Inlet tube	3800	4600	6500
Position 1 (in)			
1	3200	3800	5600
2	3200	3000	4100
3	3600	2100	2000
5	1000	1600	900
Position 2 (in)			
1	1500	2200	1700
3	1500	1800	2200
5	0	1000	1600
7	0	0	1000
Position 3(in)			
1	1500	1100	1200
2	1000	1400	1400
3	800	1200	1400
5	1500	1000	1300
Outlet (in)			
1	2600	3000	2800
Focus 2	3000	3300	3300
Wall 2	3000	2700	2700

12.3 B.3: Axial-Dowel Wheel Separator

Air velocity profiles for the Axial-Dowel Wheel Separator are described below. Measurements were taken at the positions shown in Figure B.41.

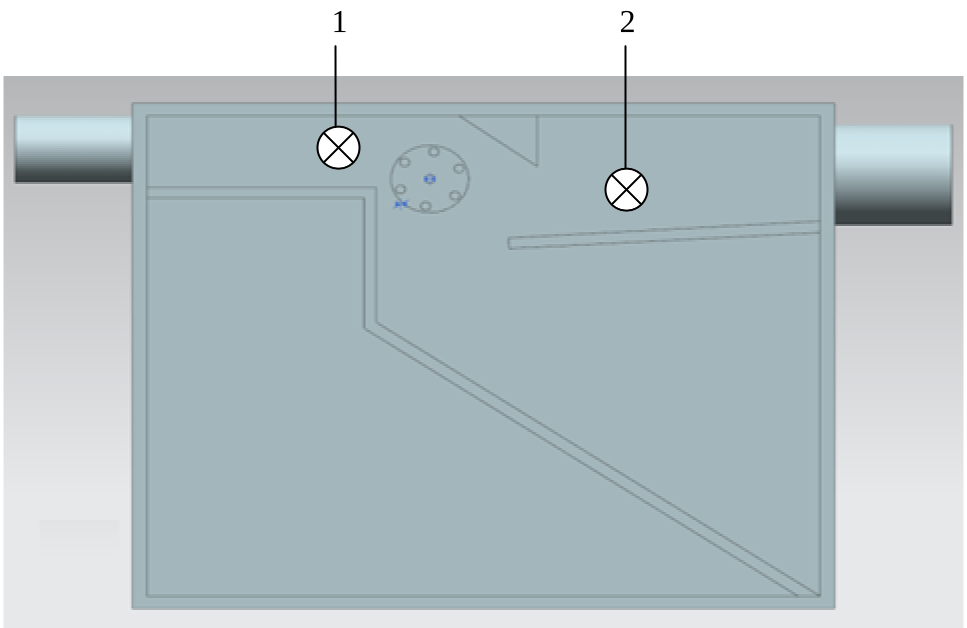

Figure B.41. Axial-Dowel Wheel Separator air velocity measurement positions.

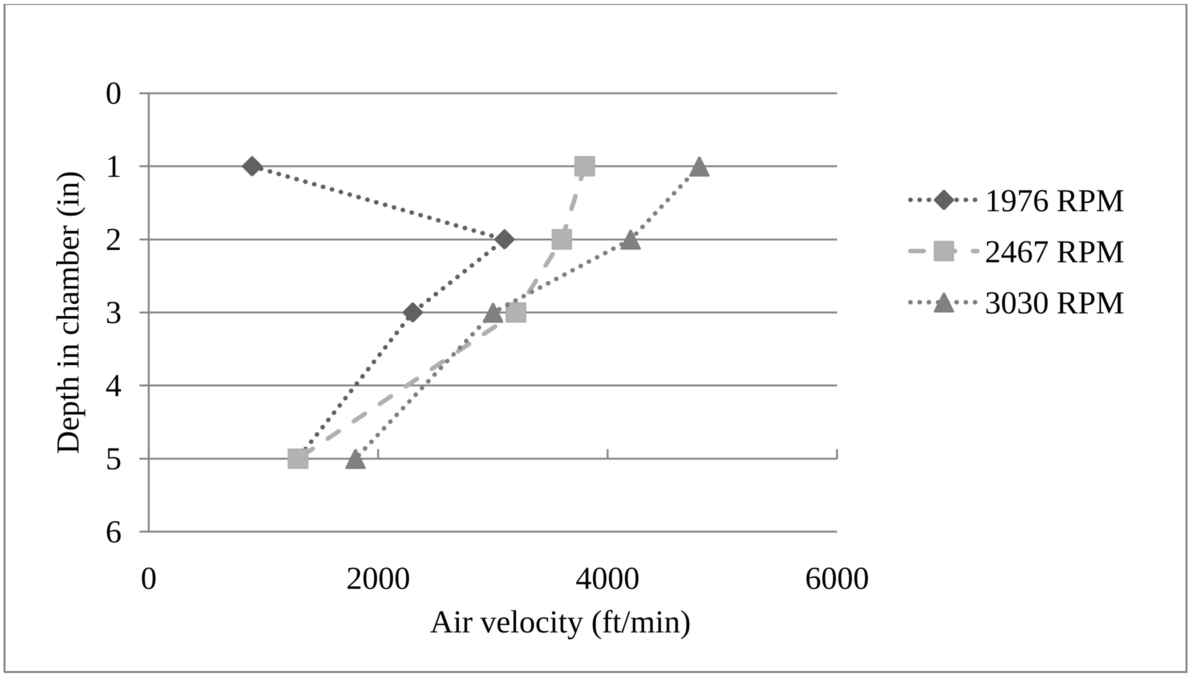

Figure B.42. Axial-Dowel Wheel Separator air velocities at position 1.

The air profile layers in the Axial-Dowel Wheel Separator at position 1 are shown in Figure B.42. The profile for each air layer is similar in the bottom 3 inches of the chamber.

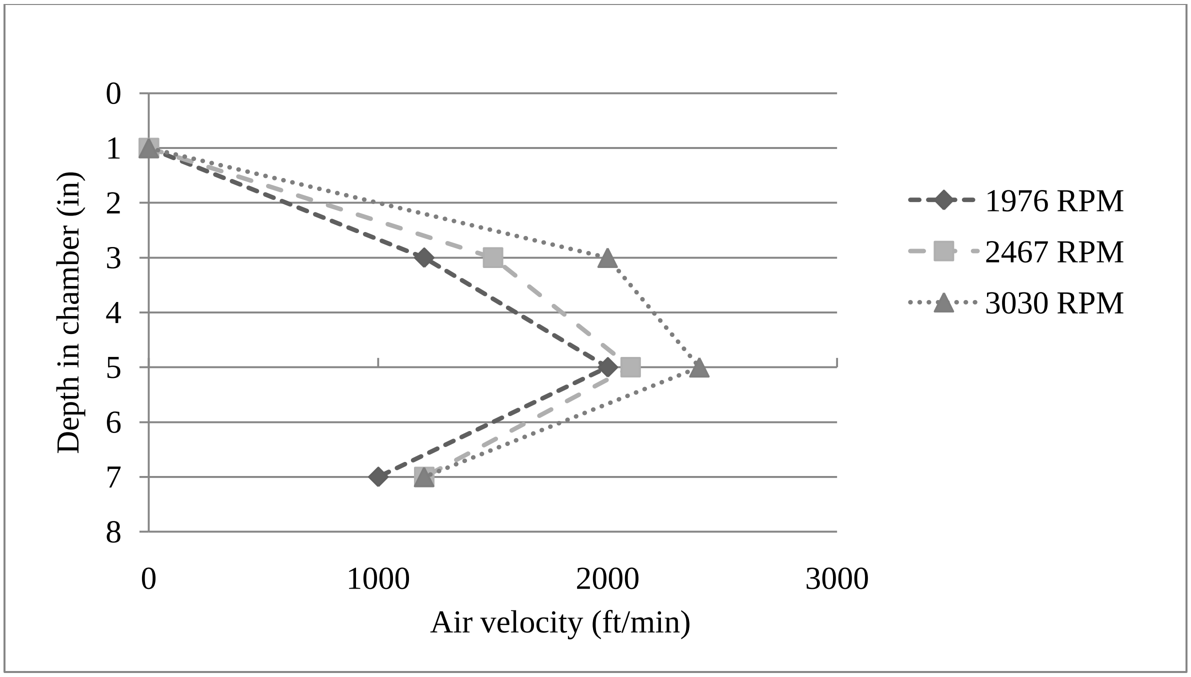

Figure B.43. Axial-Dowel Wheel Separator air velocities at position 2.

Table B.18. Axial-Dowel Wheel Separator air velocities.

Engine shaft RPM	1976	2467	3030
Fan Shaft RPM	1222	1471	1816
	Velocity Measurements (ft/min)		
Focus Inlet tube	3200	4300	5600
Position 1 (in)			
1	900	3800	4800
2	3100	3600	4200
3	2300	3200	3000
5	1300	1300	1800
Position 2 (in)			
1	0	0	0
3	1200	1500	2000
5	2000	2100	2400
7	1000	1200	1200
Outlet (in)			
Focus 1	2500	3000	3700
Focus 2	3300	3700	4600
Wall 2	2100	3500	4200

12.4 B.4: Radial-Dowel Wheel Separator

Air velocity profiles for the Radial-Dowel Wheel Separator were assumed to be similar to the profiles gathered in the Axial-Dowel Wheel Separator because the boundary planes did not change geometry in the conveying region between the two designs.

12.5 B.5: Deflection Separator

The air velocity profiles for the Deflection Separator were not taken in this experiment. The deflectors described in the design of the Deflection Separator were mounted in the middle of the air flow chamber, preventing consistent measurement positions between the previous designs.

12.6 B.6: Saltation Sieve Separator

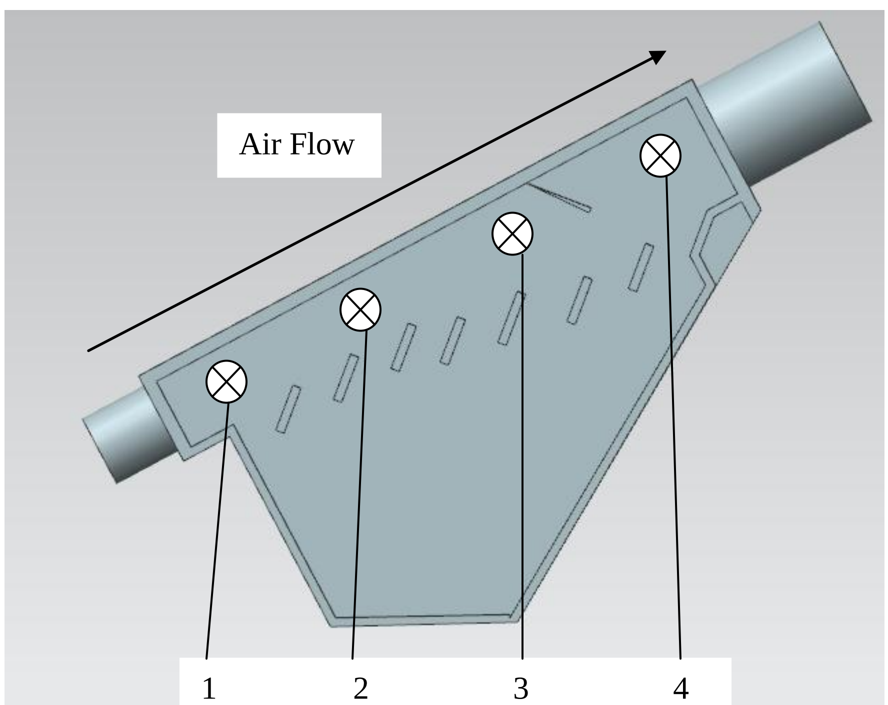

Figure B.44. SSS air velocity measurement positions.

Air velocity profiles were collected within the SSS system at the positions shown in Figure B.44. One of the benefits of the hinged paddle is: it influences the air layer to remain towards the bottom of the conveying region, yet will open when a large amount of debris, or plug flow, is present. This design ensures that the material will be conveyed along the momentum skids.

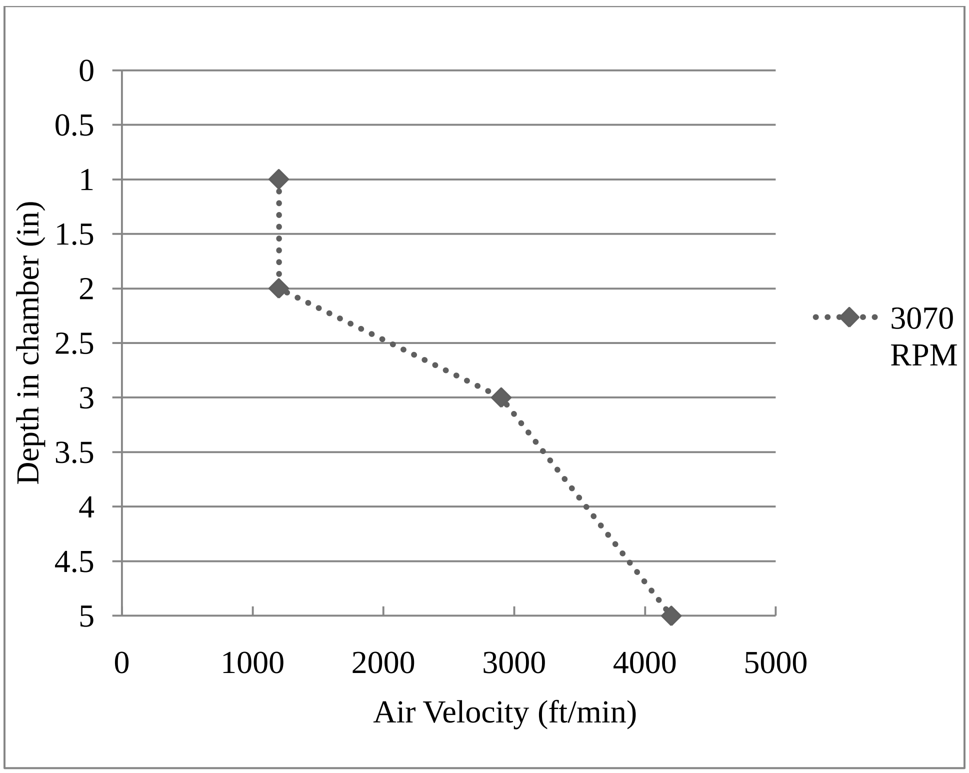

Figure B.45. SSS velocity profile at position 1.

The maximum velocity of the air stream at position 1 is shown in Figure B.45, and is located in the bottom half of the tube. Airflow can pass through the paddle, effectively slowing the airflow directly downstream from it, or at the top of the conveying region. A higher velocity airstream, just above the momentum skids, will help move any bed formation that might occur when material is entering the SSS system.

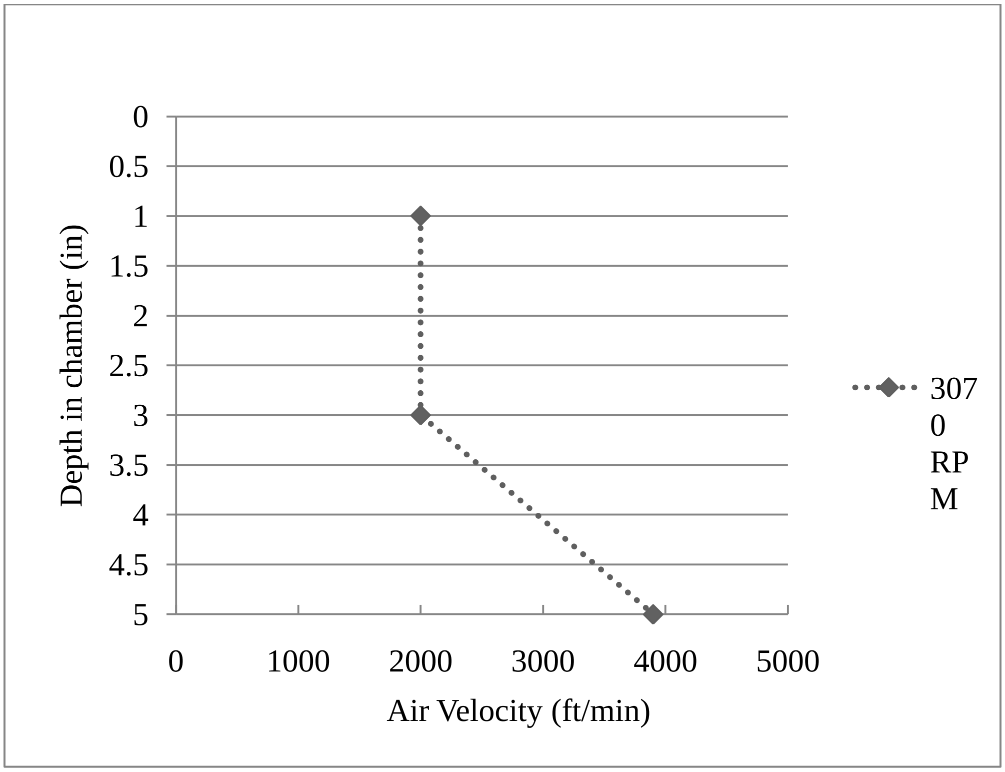

Figure B.46. SSS velocity profile at position 2.

At position 2, the air profile again shows a maximum velocity in the bottom half of the conveying region. Position 2 is located above the second momentum skid from the inlet side.

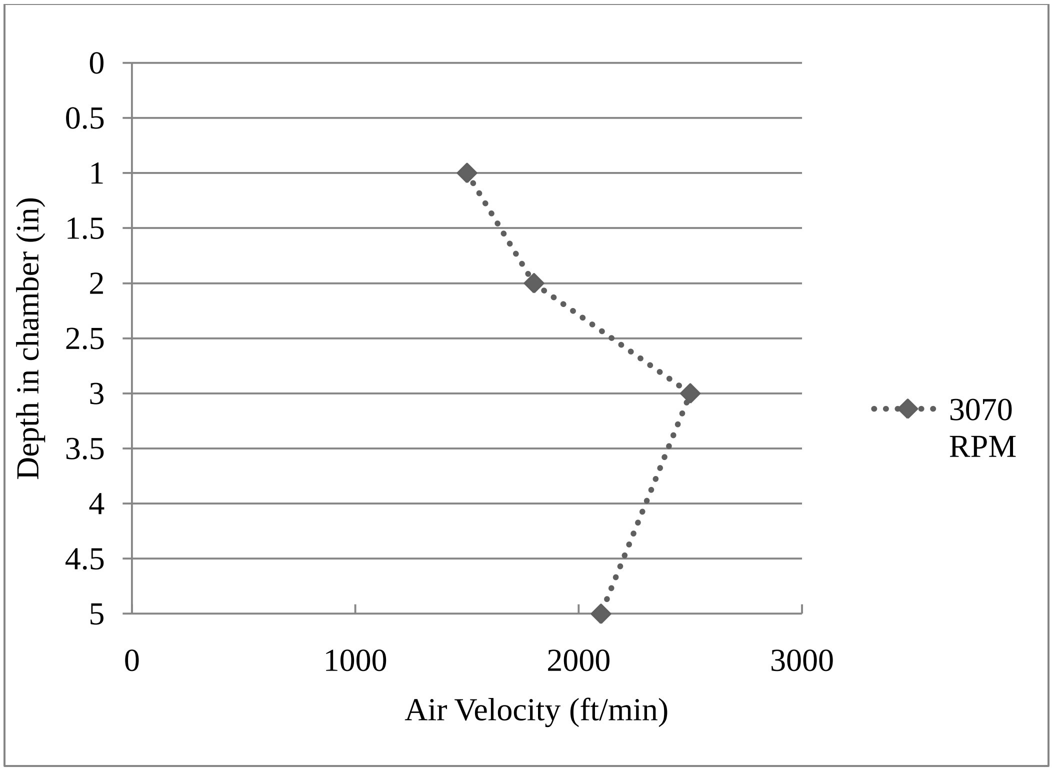

Figure B.47. SSS velocity profile at position 3.

Position 3 is located 4 in. upstream from the hinged paddle. The maximum velocity has begun to shift through the artificial orifice created between the paddle and the transfer skids, shown in Figure B.47. This desired effect produces a smaller air stream directly above the transfer skids. A faster moving air stream above the transfer skids helps ensure material movement while sorting from the bottom.

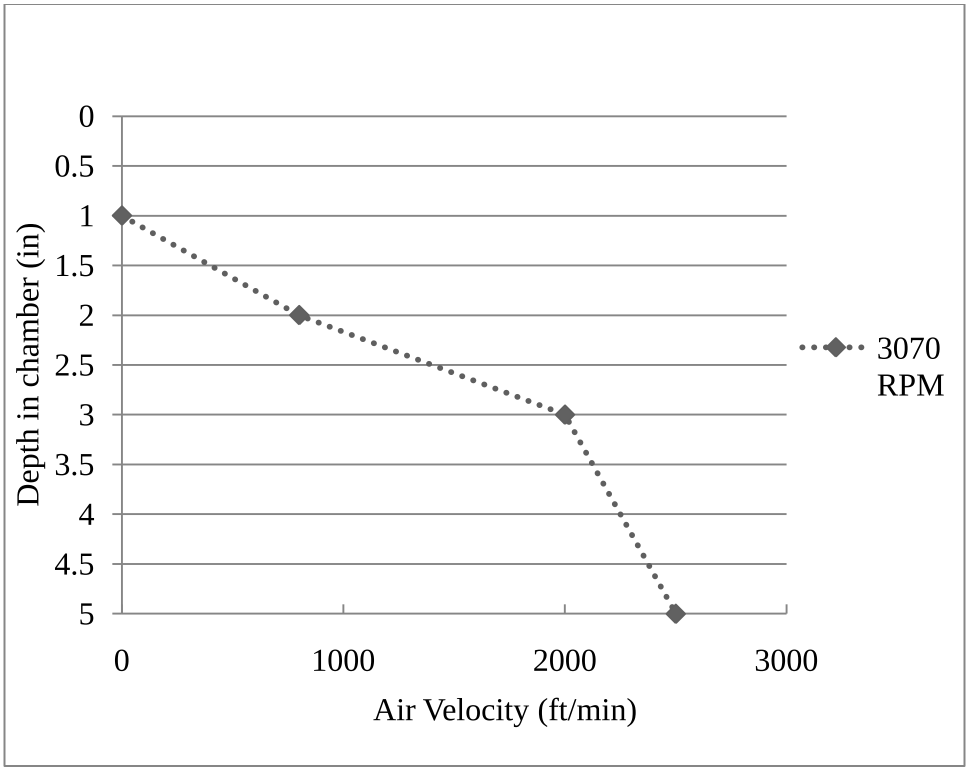

Figure B.48. SSS velocity profile at position 4.

Interactions were designed to change the momentum of the chestnuts and also to lessen the impact forces commonly associated with fruit damage; angling the momentum skids while hinging the paddled minimizes the perpendicular impacts. It is assumed that a perpendicular

Table B.19. Momentum Transfer Separator air velocity measurements.

Engine shaft RPM	3070
Fan Shaft RPM	1822
	Velocity Measurements (ft/min)
Focus Inlet tube	5400
Position 1 (in)	
1	0
2	1200
3	2900
5	4200
Position 2 (in)	
1	2000
3	2000
5	3900
7	1400
Position 3(in)	
1	1500
2	1800
3	2500
5	2100
Position 4(in)	
1	0
2	800
3	2000
5	2500
Outlet (in)	
1	3600
Focus 2	4500
Wall 2	3700

REFERENCES

Baker, K. D., R. L. Stroshine, G. H. Foster and K. J. Magee. 1984. Performance of a pressure pneumatic grain conveying system. ASAE Paper No. 84-3515, ASAE, St. Joseph, MI 49085.

Cernusca, Ina. Fall 2009. U.S. Chestnut Import Trends. *The Chestnut Grower*, Vol 11. No. 4 (4).

Coates, W., Lorenzen, B. 1990 Equipment for Ground Harvesting Jojoba seed. *American Society of Agricultural Engineers*. Vol 6(2):March 1990.

Guyer, D. E., Kang, W., Development of Chestnut Harvesters for Small Farms. Printed article. 2009.

Henderson and Perry., Agricultural Process Engineering. New York, John Wiley and Sons, Inc. 1955.

Langhaar, Henry L., Dimensional analysis and theory of models. New York, John Wiley and Sons Inc. 1951.

Lapple, C. E. and C. B. Shepherd (1940). Calculation of particle trajectories. Industrial and Engineering Chemistry. Vol 32:605-617. 1940.

Kepner, R. A., Bainer, R., Barger, E. L., (1972). Principles of Farm Machinery. Westport, CT. The AVI Publishing company inc.

Klenin, N. I., Popov, I. F., Sarun, V. A., (1985). Agricultural Machines. New Delhi, India. Amerind Publishing Company.

Kraus, M. N., (1968). Pneumatic Conveying of Bulk Materials. New York, NY. The Ronald Press Company.

Marcus, R. D., Leung, L. S., Klinzing, G. E., Rizk, F., (1990). Pneumatic conveying of Solids: A theoretical and Practical Approach. New York, NY. Chapman and Hall.

Mizrach, A., A. Zaltzman, G. Manor and Z. Nir. 1984. Gravitational motion of spheres in a fluidized bed. TRANSACTIONS of the ASAE 27(6):1674-1678.

Mohsenin, Nuri, N. 1970. Physical Properties of Plant and Animal Materials. New York, N.Y.: Gordon and Breach, Science Publishers, Inc.

Myers, Raymond H., Montgomery, Douglas C., Anderson-Cook, Christine M. (2009). Response Surface Methodology: Process and Product Optimization Using Designed Experiments. 3rd ed. New Jersey.

Patzlaff, A. W. 1980. Hydrodynamic blueberry sorting. U.S. Patent No. 4225424.

Quackenbush, Harold E., Pneumatic fruit harvesting and associated fruit characteristics. M.S. Michigan State University. 1961. Print.

Shen, L., Haque, E., Posner s., 1994. Saltation Velocity of Wheat Material in Horzontal Flow. *Transactions of the ASAE: American Society of Agricultural Engineers*: VOL. 37(2):577-580, print.

Shortley and Williams. Principles of college physics. Prentice-Hall. Englewood cliffs, NJ. 1959.

Srivastava, A. K., Goering, C. E., Rohrbach, R.P., Buckmaster, D. R., Engineering Principles of Agricultural Machines. 2nd Edition Chapter 1, pp. 1-14. American Society of Agricultural and Biological Engineers technical library.

Srivastava, A., VanEe, G., Ledebuhr, R., Welch, D., Wang, L., Design and Development of an Onion-Peeling Machine. *Applied Engineering in Agriculture, American Society of Agricultural Engineers (*1997): VOL. 13(2):167-173

United States Department of Agriculture. 2007. Census of Agriculture: Summary and State Data. Volume 1: Geographic Area Series, Part 51. Printed Article.

Van Ee, G. R., Haffar, I. "A Model to Describe Terminal Velocities of Graded Cucumbers". *Journal of American Society of Agricultural Engineers* (1990):Vol 6(2) Print.

Yildiz, M. U., Ozcan M. M., Calisir S., Demir F., Er F., 2009. Physico-Chemica Properties of Wild Chestnut Fruit Grown in Turkey. *World Applied Sciences Journal* 6(3): 365-372,2009.

Zaltzman, A., Schmilovitch, Z. 1986. Evolution of a Potato, Fluidized Bed Medium Separator. ASABE technical libray.

Zaltzman, A., Z. Schmilovitch and A. Mizrach. 1985. Separating flower bulbs from clods and stones in a fluidized bed. Canadian Agricultural Engineering 27(2): 63-67.

Zaltzman, A., A. Mizrach and Z. Schmilovitch, 1986. Analytical model of a gravitational separation process in fluidized bed medium. Journal of Agricultural Engineering Research 34(4):257-273.

Zaltzman, A., R. Feller, A. Mizrach and Z. Schmilovitch. 1983. Separating potatoes from clods and stones in a fluidized bed medium. TRANSACTIONS of the ASAE 26(4): 987-990, 995.

Zaltzman, A., A. Mizrach and Z. Schmilovitch. 1982. Fluidized bed separator. United States Patent No. 4,322,287.